Journal of Archaeological Science 41 (2014) 89–105

Contents lists available at ScienceDirect

Journal of Archaeological Science

journal homepage: http://www.elsevier.com/locate/jas

Technology, production and chronology of red window glass in the medieval period – rediscovery of a lost technology

Jerzy J. Kunicki-Goldfinger [a], Ian C. Freestone [b,*], Iain McDonald [c], Jan A. Hobot [d], Heather Gilderdale-Scott [e], Tim Ayers [e]

[a] Institute of Nuclear Chemistry and Technology, Dorodna 16, Warszawa 03-195, Poland
[b] Institute of Archaeology, UCL, 31-34 Gordon Square, London WC1H 0PY, UK
[c] School of Earth and Ocean Sciences, Cardiff University, Main Building, Park Place, Cardiff CF10 3YE, Wales, UK
[d] Electron Microscopy Unit, School of Medicine, Cardiff University, Cardiff CF14 4XN, Wales, UK
[e] Department of History of Art, University of York, Heslington, York YO10 5DD, UK

ARTICLE INFO

Article history:
Received 24 December 2012
Received in revised form
24 July 2013
Accepted 25 July 2013

Keywords:
Glass technology
Stained glass window
Medieval
Red glass
Ruby glass
Copper nanoparticle
York Minster
Glass composition
Scanning electron microscopy
Transmission electron microscopy
Energy dispersive X-ray analysis
Laser ablation inductively-coupled plasma mass spectrometry

ABSTRACT

SEM-EDXA of 132 examples of medieval red window glass reveals the presence of around 1% copper oxide in all cases. SEM and TEM of selected samples confirm the presence of Cu nanoparticles. Two structural categories of red glass sheet are identified. Sheets comprising a single layer of red glass from a few tens to around 300 μm thick overlying a supporting substrate of white glass, with or without a protective cover of white glass, are typically found from the fourteenth century onwards. However, in 12th–14th century England, France and Spain, and perhaps elsewhere, typical red glass sheets have a complex microstructure comprising multiple coloured striae about 1 μm thick in a white background. SEM–EDXA, TEM and LA-ICP-MS have been used to characterise and investigate the technologies of the two types in detail. The single-layered glasses were produced using an approach analogous to that of copper red glass in the modern period, where a red glass is flashed onto a colourless base. In contrast, the multi-layered glasses were formed by the incomplete mixing of an oxidised high-Cu and a reduced low-Cu glass. The red colour forms due to the diffusion of oxidised copper into the reduced glass and the nucleation and growth of metallic copper during heat-treatment. This represents a previously unrecognised medieval glass technology, where red was created by mixing two weakly coloured glasses, a complex, arcane and mysterious procedure which must have reinforced the exclusivity of the craft. The occurrence of the technique has implications for dating windows and the identification of glass which has been inserted in early restorations and repairs, for the trade in coloured glass and for the transfer of glassmaking technologies in medieval times. It provides a link between stained glass window technology of the high medieval period and the glass-colouring practices of the late first millennium CE.

1. Introduction

Stained glass constitutes one of the most characteristic features of medieval church architecture and is an important source of medieval imagery. With origins in the first millennium AD (Cramp, 2001; Goll, 2001; Whitehouse, 2001 and other papers in Dell'Acqua and Silva, 2001) figurative glazing with coloured glass spread across much of Europe in the 12th century. Shaped pieces of coloured glass were joined with H-section lead *cames* to create representations of religious scenes or simpler, non-figurative panels which enhanced the spiritual experience by filling the building with light and colour.

Translucent red constituted an important component of the medieval glazier's palette (Fig. 1) and is one of a number of distinctively medieval technologies in the manufacture of glass windows, which include silver stain and grisaille painting. However, the manufacturing processes used to produce these *ruby red* glasses represent some of the least well understood aspects of medieval glass technology. With the exception of a rare group of late Roman glass vessels, of which the Lycurgus Cup is the best known (Barber and Freestone, 1990), virtually all known examples of earlier red glass are opaque (Freestone, 1987; Brill and Cahill, 1988; Brun et al., 1991; Freestone et al., 2003; Barber et al., 2009; Verità and Santopadre, 2010); the routine production of translucent red glass was a medieval European achievement. Furthermore, the scale of production was huge: Wedepohl (2003, 2010) has estimated that in Central Europe alone, some 40 000 tonnes of glass

* Corresponding author. Tel.: +44 (0)2076797498.
E-mail address: i.freestone@ucl.ac.uk (I.C. Freestone).

0305-4403/$ – see front matter © 2013 Elsevier Ltd. All rights reserved.
http://dx.doi.org/10.1016/j.jas.2013.07.029

Fig. 1. Panel 8e from the Great East Window (1405–1408) at York Minster, showing the Army of the Horsemen, described in Revelations ix: 16–19 (Photograph the York Glaziers Trust, reproduced courtesy of the Chapter of York).

were produced between A.D. 1250 and 1500, and a significant part of this production was window glass. Translucent red constituted a significant element of that production, as may be seen from the surviving examples in medieval cathedrals.

The detailed mechanisms of production of red colour in medieval glass are not well understood. However, there is a consensus among modern investigators that ruby red colouration in medieval window glass is due to the presence of nanoparticles of metallic copper (Knowles, 1927; Nakai et al., 1999; Fredrickx, 2004; Farges et al., 2006; Colomban et al., 2009). The transmission of light by such glasses is low and, in the thickness of a typical window pane, they appear dark or opaque. To obtain a translucent ruby colour, all known medieval translucent reds, as well as many modern translucent red glasses, comprise at least two layers, where a thin layer of red glass is laid over a thick supporting layer of colourless or weakly coloured glass. Following art-historical convention, we will use the term "white" to encompass the range of colourless and unintentionally very pale blue, green and yellow glasses that form the substrate or support.

In the modern world, red window glass has conventionally been produced by a glass-working technique known as flashing, where a gather of molten white glass is taken on the end of a blowing iron then dipped into a pot of a colour (or vice versa). The composite gather is then blown into a cylinder of glass with a thin layer of colour on one surface. The expansion of surface area as the glass is blown can result in the development of a very thin coloured layer over a sheet of glass just a few millimetres thick. The layered glass cylinder is then cut and opened up while hot to form a flat sheet of coloured glass.

Copper may exist in glass as cuprous ions (Cu^{+}), which are virtually colourless, and as cupric ions (Cu^{2+}), which typically produce a pale blue or green colour, dependent upon the composition of the glass matrix (Weyl, 1951). The equilibrium between them, hence the colour of the glass, is controlled by the partial pressure of oxygen:

$$2Cu^{+} + O_2 = 2Cu^{2+} + O^{2-} \quad (1)$$

Oxidising conditions favour the blue-green colour. When conditions are sufficiently reducing, however, copper metal may form and, as its solubility is low, it will precipitate from the glass:

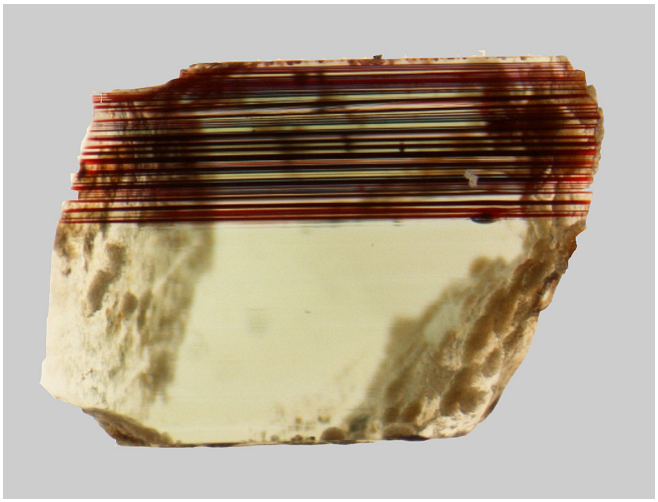

Fig. 2. Striated structure (Type A). Panel 1a, window CHn9, York Minster (c. 1290–1300). Glass thickness c. 2.8 mm.

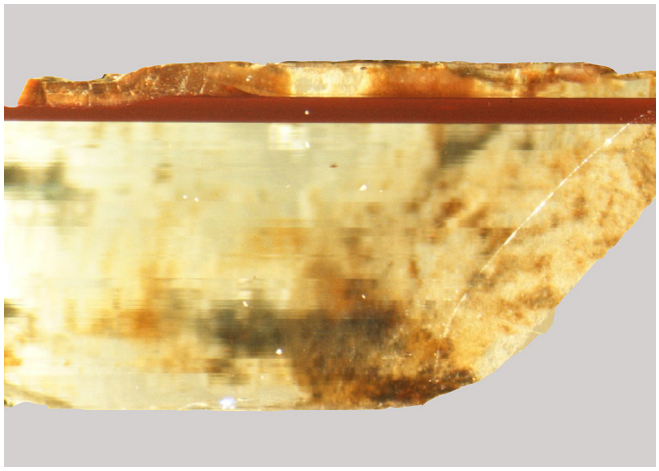

Fig. 4. 3-layer structure (Type B-3), with additional layer of white ('coperta') overlying the red. Panel 2b, Great East Window, York Minster (1405–1408). Glass thickness c. 2.7 mm. (For interpretation of the references to colour in this figure legend, the reader is referred to the web version of this article.)

$$Cu^{+} + e^{-} \rightarrow Cu^{0} \quad (2)$$

If the particles of metallic copper formed in this way are sufficiently small (in the order of tens of nanometres) and widely spaced, then a translucent ruby red glass may be developed.

Medieval copper red glass has attracted the attention of various researchers but the first detailed scientific study was that of Martha Spitzer-Aronson who, in a series of papers (Spitzer-Aronson, 1974, 1975, 1976, 1977, 1978a, 1978b, 1979, 1980, 1989) drew attention in particular to the occurrence of multiple layers of red, as opposed to a single layer, which are not readily explained by the simple flashed glass model. Many of the issues addressed by Spitzer-Aronson remain unresolved and her work is under-referenced in the modern literature. Later studies, cited above, have confirmed the role of copper in colour generation but have paid less attention to the compositional and micromorphological evidence, which provide crucial information on the technological practices of the glassmakers, and their variation in space and time.

The present paper forms part of an investigation of a large sample of medieval window glass, focussing on York Minster in northern England, but including glass from elsewhere in Britain as well as from continental Europe (Freestone et al., 2010). It is shown that medieval "flashed" red glass falls into two fundamentally different micromorphological types and their occurrence shows evidence of systematic chronological variation, a possibility originally suggested by Winston (1847: 22) and later by Spitzer-Aronson (1974, 1975) but subsequently untested. These characteristics reflect fundamentally different approaches of the craftsmen to the generation of the red colour, which are likely to reflect their empirical understanding and their ability to control the systems with which they worked. It is shown that, between the 12th and 14th centuries at least the red glass used in France, England, and Spain was produced in a way which has been previously unanticipated and which is unparallelled in other technological traditions.

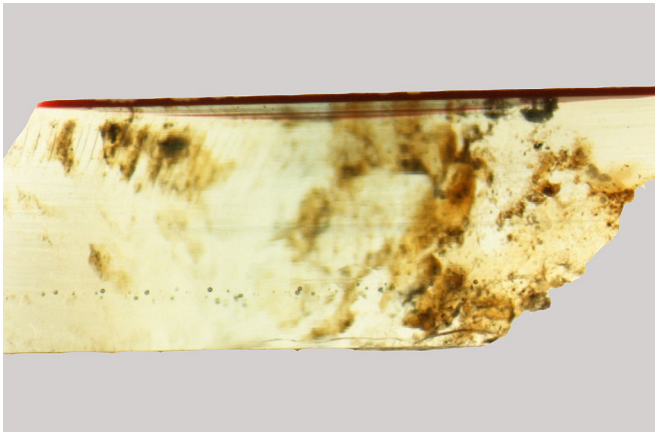

Fig. 3. 2-layer structure (Type B-2), showing a single layer of red glass overlying a white substrate. Panel 2e, Great East Window, York Minster (1405–1408). Glass thickness c. 1.9 mm. (For interpretation of the references to colour in this figure legend, the reader is referred to the web version of this article.)

2. Materials and methods

One hundred and thirty-two ruby red window glasses from windows covering the period from the twelfth to the sixteenth centuries were examined. Most of them originate from English churches, including forty-eight from York Minster. However the sample includes glass from windows in France, Germany, and the Netherlands as well as a single example from Spain. Sample contexts and dating are presented in Table 1.

Where possible samples were removed from windows undergoing conservation, to ensure robust contextual control, but others are fragments which had not been replaced when the windows were restored, and which were retained by the conservator and/or the custodians. The Dutch glasses are from archaeological deposits and a few others are from museum collections. All glasses discussed have been carefully described and their context, history and location within the panels/windows/sites established as far as possible.

The glass fragments were sampled using a diamond tool and the sampling positions were carefully described and documented using digital photography. The samples were embedded in an artificial resin and polished with diamond pastes down to 0.25 μm grade to reveal as far as possible the complete cross-sections of the original glass sheets. Due to the variable state of preservation, in a few cases only a part of the cross-section could be revealed.

A Nikon SMZ1000 zoom stereomicroscope with a CoolPix 4500 digital camera attachment and a Nikon Eclipse ME600 Research Microscope with a Nikon DS digital camera were used to investigate the structure and morphology of the glass surface as well as of its

Table 1
Red glass samples examined in the present study: contexts, dating and number of samples.

Original locations context/collection	Dating of the window/panel or site	No.	Art historical comments	Typology of glass structure
St. Denis, France. Victoria & Albert Museum, London [panel with geometric-floral decoration, c. 63–1989]	12th century	7	Composite panel(s)?	Type A
York Minster, York, England. Nave Clerestory (Tracery), various panels	12th century	6	Dating of 3 red glass fragments from the Medallion Panel is uncertain	Type A
Westminster, England. Loose piece, lack of data	Mid-late 13th century	1	–	Type A
Burgos cathedral, Burgos, Spain. Loose piece, lack of data	13th century	1	–	Type A
York Minster, York, England. Chapter House, Vestibule, window n9 and s7, various panels	c. 1290–1300	12	11 items described as either original or contemporary to original/panel. 1 glass described as a 'stop gap'	Type A (10 samples) Type B-3 ('modern' insert) 1 original unclassified sample
Swabia (Esslingen?), Germany. Panel with Tree of Jesse, Museum of Architecture, Wrocław, Poland [Dep. 46]	1st quarter of the 14th century	1	–	Type B-3
Cologne cathedral, Germany. Windows in the Choir ambulatory chapels or possible from choir clerestory. Loose pieces. Cologne cathedral depo.	Around 1330/40	3	–	Type B-3 (1 sample) Type B-2 (2 samples)
Wells Cathedral, Wells, England. British Museum [Group 1, 36469Q (BMRL no) Box 1]	Possible 14th century	1	Acquired from the British Museum collection of samples	Type A
Chapter of New College, Oxford, England. Window n5, panels B2 and D2	c. 1385	13	–	Type B-3 (8 samples) Type B-2 (5 samples)
Cistercian Abbey of Altenberg (near Cologne), Germany. Westfenster – West I and Nordfenster – unknown location. Loose pieces. Oidtmann's (Linnich) depo	1386–1397	5	Dating of 2 items from Nordfenster unknown	Type B-3 (1 sample) Type B-2 (4 samples, including 2 of unknown dating from Nordfenster)
Canterbury cathedral, Canterbury, England. Chapter House, window w1, tracery. Loose pieces	1396–1399?	3	–	Type A
York Minster, York, England. The Great East Window, various panels	1405–1408	21	Original/possible original or contemporary to original, in a few cases - no remarks. 1 glass possible 14th century and 1 insert	Type B-3 (10 samples) Type B-2 (7 samples) Type A (1 item, possible 14th century) Type B2 (3 sample, 'modern' inserts)
York Minster, York, England. Saint William Window, various panels	c. 1415	9	Original glasses	Type B-3 (3 samples) Type B-2 (6 samples)
Coventry Cathedral, England. Coventry Cathedral store, loose pieces	Beginning of the 15th century	3	One glass attributed to Thornton, one described as a contemporary to Thornton and one as medieval	Type B-3 (2 samples) Type B-2 (1 sample)
Domestic chapel of Hampton Court, Herefordshire, England. Window with Eight Apostles, the Pietà, and other saints. Various panels. Museum of Fine Arts, Boston, USA. [MFA 25.213]	c. 1420–1435	6	Original glasses	Type B-3
Church of St. Mary, Fairford, England. Window nVIII and sVI, various panels	1500–1515	17	Original glasses	Type B-3 (15 samples) Type B-2 (2 samples)
Presbytery in the centre of Heemskerk, Holland. Collection of Archeologische Wergroep Beverwijk-Heemskerk, Holland. [inv. no. of the site - HSK 18]	15th century – before 1572–73	1	Archaeological deposits	Type B-3
Church, Dieserstraat, Zutphen, Holland. Collection of Gemeente Zutphen, Holland. [Code: DS 74–80]	1300–1572	17	Archaeological deposits, most probable mid 16th century	Type B-3 (7 samples, possible 16th century) Type B-2 (9 samples, possible 16th century) Type A (1 sample, possible 14th century)
St. Catherine Church in Oppenheim (near Mainz), Germany. Nave windows, tracery panels. Loose pieces. Oidtmann (Linnich) Conservation Studio	1320–1340	5	3 samples from north window IX, tracery panel 1C	Type B-2 (all 5 samples are 'modern' inserts')

cross-section at various magnifications. The thicknesses of the fragments and dimensions of components such as flashed layers were measured using EclipseNet and SPOT RT interactive image analysis softwares respectively.

The embedded and polished samples were coated with a thin layer of carbon and analysed using a CamScan Maxim 2040 scanning electron microscope. Bulk compositions were determined with an Oxford Instruments ISIS or INCA energy dispersive X-ray spectrometer (SEM-EDS). Back-scattered electron (BSE) imaging was used to identify compositional changes and X-ray maps and line scans were used to visualize the distribution of selected chemical components.

For quantitative elemental analysis, the electron beam was typically rastered at a magnification of 500× over an area of fresh glass for 100 s, at 20 kV accelerating potential. For the analysis of small areas of interest, the electron beam was rastered at high magnification or used in spot mode. Count-rate on metallic cobalt was around 4000 cps. Standards were pure oxides and minerals and quantification was carried out using the ZAF method. Oxide weight percents were calculated stoichiometrically. Analytical totals were typically between 98% and 102% and have been normalised to 100% for comparative purposes. Corning glass D (Brill, 1999; Vicenzi et al., 2002) and the European Science Foundation medieval glass reference standards prepared by Pilkington Glass

under the direction of R.G. Newton (1977) were used as secondary standards. Good agreement between recommended and analysed results was obtained in the case of all components, except SO_3, which is close to the limits of detection. The departures from the accepted values for other elements fall below 6% relative and for CaO and SiO_2 below 1%.

To visualise the copper nanoparticles, a few samples were examined in back-scattered mode at magnifications in excess of ×50,000 in an FEI XL30 environmental SEM with field emission gun (FEG), operated at high vacuum at 20 kV accelerating potential and 10 mm working distance. Elemental compositions were determined with an Oxford Instruments INCA energy dispersive x-ray system (EDS). Two selected samples were also examined at magnifications up to 88 000 in a Philips CM12 transmission electron microscope (TEM), operated at 80 kV, and fitted with an EDAX Genesis elemental analysis system. TEM sample preparation was based upon the method of Roe et al. (2006). The glasses were ground down to expose the red, and fragments selected in an optical microscope so that as far as possible only areas with red pigmentation were present. The red glass was then crushed and small particles were suspended in acetone. Small droplets of suspension were placed on carbon film on 200 mesh gold grids (Agar Scientific, S160A) and air dried for observation in the TEM.

Selected polished samples were analysed for trace elements using Laser Ablation Inductively-Coupled Plasma Mass Spectrometry (LA-ICP-MS).

Over 40 elements were analysed using a New Wave Research UP213 laser system coupled to a Thermo X Series2 quadropole ICP-MS system. For analysis the laser was operated a frequency of 20 Hz, using a 40 μm spot size that delivered ~6.7 Jcm^{-2} of energy along a line pattern with the sample moving at 6 microns per second relative to the laser. The layer of carbon was removed from each sample before analysis and a pre-ablation (4 Hz delivering ~0.05 Jcm^{-2}) was carried out prior to the main ablation in order to remove any surface contamination. Mass spectrometry was performed in time-resolved analysis (TRA) mode using isotope dwell times ranging from 2 ms for high abundance elements such as Si, to 30 ms for low abundance trace elements. Each total element scan was completed in ~750 ms and individual timeslices were compiled into a complete TRA spectrum within the Plasmalab instrument software. Portions of the TRA spectrum showing the most stable and consistent profiles were selected for integration. Calcium concentrations that had been determined previously by SEM-EDS were used for internal standardisation. NIST glasses 614, 612 and 610 were used as primary calibration standards (Gao et al., 2002), with Corning Glass D used as an external standard.

A number of experiments were carried out specifically to collect time resolved line profiles across different zones within a single sample of glass. For these experiments the laser spot was reduced to 12 μm and the laser frequency reduced to 15 Hz. This produced fewer counts overall and increased the detection limits compared to the quantitative analyses by a factor of about 10. However, it reduced the signal variation and produced smoother profiles that highlighted the changes between the different zones. The motion of the samples under the laser beam was reduced to 1 μm s^{-1} to increase the resolution of the profiles (linescans). The other parameters remained the same.

3. Results

The great majority of white base glasses analysed are of the potash-lime-silica type with 45–60% SiO_2, 10–27% CaO and 3–27% K_2O and with P_2O_5 and MgO in the ranges 0.7–6.8% and 2.5–8.5% respectively. This composition is characteristic of so-called forest glass of the medieval period, melted using wood ash as a source of flux (e.g. Wedepohl, 2003, 2010). Of the examined samples, nine were clearly identified as post-medieval on the basis of major element composition. For example, some were soda–lime–silica glasses with low chlorine, indicating that they were made after the introduction of the Leblanc process in the early nineteenth century on a wide scale (Clow and Clow, 1952; Chopinet, 2004), while others were alkali–lead–silica glasses with low contents of impurity. These were categorised as modern insertions into the windows (i.e. repairs) and are not further considered in detail.

Although they are all potash–lime–silica glasses, the medieval flashed reds do not constitute an entirely homogenous group with respect to chemical composition. Two major subgroups may be distinguished, based on CaO and MgO concentrations (Fig. 5; Freestone et al., 2010). These Low Lime High Magnesium (LLHM) and High Lime Low Magnesium (HLLM) groups are clearly distinguishable within glasses of a single region, particularly the UK, where most of our sampling has been conducted. However, as glasses from a wider region are included, some overlap becomes apparent, due to the diversity of sources on the one hand and our inability to date accurately each individual fragment of glass on the other. The subdivision between Low Lime High Alkali (LLHA) and High Lime Low Alkali (HLLA) glasses has been widely used in the literature, and these categories correspond more-or-less to our own LLLM and HLLM, but we do not consider them appropriate for our period of study, as glasses in the two groups we recognise may contain similar concentrations of total alkali, in excess of 10% $K_2O + Na_2O$. SEM-EDS analyses for major elements with, where quantified, LA-ICP-MS data for copper are provided in Inline Supplementary Table S1.

Inline Supplementary Table S1 can be found online at http://dx.doi.org/10.1016/j.jas.2013.07.029.

In the light microscope, all medieval reds are seen to comprise at least one red and one white layer. No glass sheet coloured red throughout was found. Two main structural groups were distinguished. *Type A* has a striped or *striated* structure (Winston, 1847) and is apparently characterised by many separate layers of white glass with thin red layers or striae close their boundaries, as shown in Fig. 2. This is the variety termed "fueilleté" by Spitzer-Aronson (1975). *Type B* ("plaqué") corresponds more readily to the widely understood concept of flashed glass and comprises two or three separate and easily distinguishable layers, of which only one is red. *Type B-2* comprises a simple red layer overlying a white base (Fig. 3) while *Type B-3* has an additional white layer over the red (Fig. 4). The chronological occurrence of these types in our sample is given in Table 2 and their correlation with the HLLM and LLHM groups is also strong (Fig. 5).

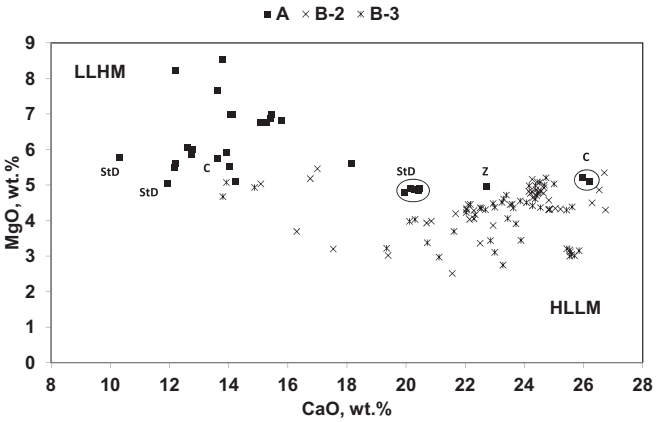

Fig. 5. Scatter plot of CaO versus MgO for 120 white supporting layers of red sheets. StD – St Denis, C – Canterbury, Z – Zutphen.

Table 2
Occurrence of Type A and Type B red glass in the examined sample, according to date and place.

	12th century ($n = 13$)	13th century ($n = 12$)	14th century ($n = 26$)	15th century ($n = 35$)	16th century ($n = 34$)	Medieval ($n = 2$)	Post-medieval/modern inserts ($n = 9$)	Total ($n = 131$)[a]
Type A	13	12	6					31
Type B			20	35	34	2	9	100
B-3			*11*	*21*	*23*		*1*	*56*
B-2			*9*	*14*	*11*	*2*	*8*	*44*
Locations								
Type A	England, France	England, Spain	England, Netherlands					
Type B			England, Netherlands, Germany	England Netherlands (?)	England, Netherlands	Germany	England, Germany	

[a] One unclassified glass not included.

3.1. Relation between structure, colour, and composition: Type A glass

All *Type A* glasses share a number of characteristics in common and we illustrate these by reference to three examples. The first is from panel 2b of the Great East Window of York Minster (project sample no. 11). The window itself dates from 1405 to 8, but the composition and position of this particular sample in the window suggest that it represents a later repair which used glass from an earlier window (see Freestone et al., 2010 for discussion of inserts in the Great East Window). The second example is from the cathedral in Burgos, Spain, dated to the 13th century (no. 844); and the third is from Canterbury cathedral, England, dated to the 14th century (no. 859). Light microscopy shows the York sample (Fig. 6), to have a series of at least ten red striae concentrated towards one surface. The tapering appearance and finite thicknesses of these striae as shown in Fig. 6 reflect the shape of the sample and the angle from which the image was taken. When viewed down their length, the red "layers" are in fact seen to be extremely thin, apparently around or less than 1 μm, a characteristic feature of all glasses of this type examined.

SEM-EDXA reveals that *Type A* glass consists of alternating layers of two white glasses which can be distinguished in high contrast back-scattered images and by X-ray mapping (Fig. 7a, b). These two glasses differ in their concentrations of copper and associated trace metals, which have high and low concentrations in alternate layers (Fig. 7b). In the example from York, CuO concentrations in the low- and high-Cu layers, as analysed by SEM-EDS, are ~0.4 and ~1.9% respectively. These concentrations are fairly typical. However, it should be noted that the measurement of Cu concentration within a layer is affected by diffusion into and out of the adjacent glass and therefore depends upon the area selected for analysis and the thickness of the layer. For eleven reds of *type A* from York Minster analysed by LA-ICP-MS, the average concentration of CuO in the low-Cu layers is 0.55% ($s = 0.39$).

Comparison of light optical micrographs with back-scattered electron images indicates that the red striae occur in the low-Cu

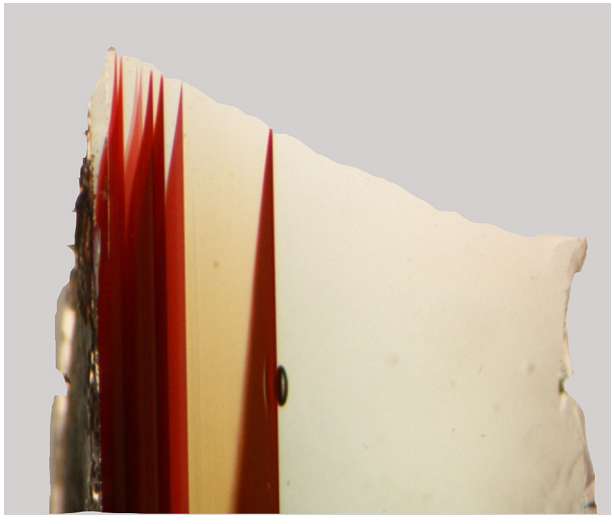

Fig. 6. Light photomicrograph of Type A glass, captured obliquely to visualise the individual red striations [Sample 11: Great East Window, York Minster, probably 14th century or earlier glass inserted as a repair]. Glass thickness c. 2.8 mm. (For interpretation of the references to colour in this figure legend, the reader is referred to the web version of this article.)

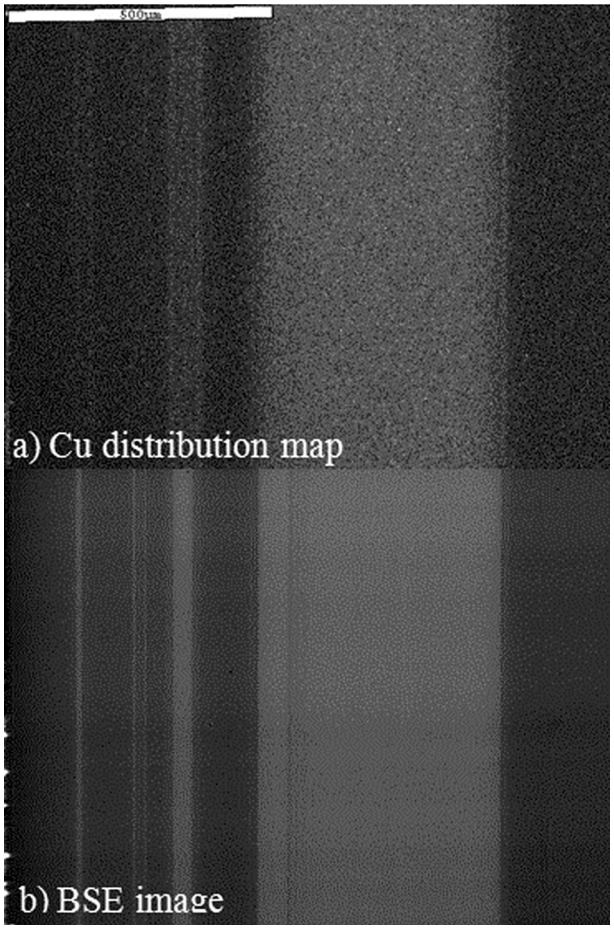

Fig. 7. a, b. SEM image of Type A glass shown in Fig. 6. a) X-ray map of Cu distribution. Lighter areas depict higher Cu concentration. b) Backscattered electron (BSE) image. Lighter areas depict higher average atomic mass (i.e. an elevated content of heavy elements).

layers, typically a few to greater than ten micrometres from the boundary with the high-Cu glass. It is emphasised that the red striae do not fill the low-Cu layers and are clearly separate from the high-Cu layers. Previous studies which imply that these glasses comprise alternate layers of red and white glass are likely to be based upon observations which are oblique to the striae, so that they appear much wider, along with a failure to precisely correlate coloured regions with compositional data.

X-ray line-scans of York sample 11, comparing the distributions of Cu and Zn, are shown relative to the back-scattered image in Fig. 8. The positions of the red striae are indicated. It is observed that very narrow peaks in Cu concentration occur in the low-Cu glass, more-or-less symmetrically on either side of the high-Cu glass. A close comparison of the image of the glass taken in the light microscope with the SEM-EDXA line-scans reveals that the peaks in copper on either side of the Cu-rich glass correspond precisely to the red striae in the glass seen under the optical microscope. Note that the line-scan for Zn shows it to be enriched in the Cu-rich glass, but it does not show maxima corresponding to the coloured striae (Fig. 8); Cu and Zn show different behaviours.

Scans using LA-ICP-MS (Fig. 9a, b) confirm and expand the findings using EDXA. Among over forty elements analysed, the concentrations (signal intensities) of only nine (Cu, Pb, Zn, Sn, As, In, Sb, Ag and Au) were found to change when moving from the low-Cu to the high-Cu glass. For all of these elements, the signal intensity was always higher within the high-Cu layer. Quantitative concentration data for the high and low copper glasses in *Type A* sample 11 from York are given in Table 3. Total concentration of this suite of metallic elements in the high-Cu layers is typically around 2% by weight element, and excluding Cu, is still around 0.8%. The total concentrations of these elements, including Cu, in the low-Cu glass is only around 0.2% by weight. However, it is re-emphasised that the concentration of Cu measured in the low-Cu glass is dependent upon the thickness of the low-Cu layer. Where the low-Cu layer is thicker, then the Cu concentration in the centre is lower; this is consistent with a process of diffusion of copper from the high-Cu glass into the low-Cu glass. When major elements are normalised (i.e. excluding copper), EDXA analyses of high- and low-Cu layers are often (but not always) identical. The differences in intensity observed in the back-scattered images of Figs. 7 and 8, for example, are due entirely to the small differences in the contents of copper and other of the associated metallic elements listed above.

The relationships of the compositional profiles to the red striations were determined by examining in optical photomicrographs

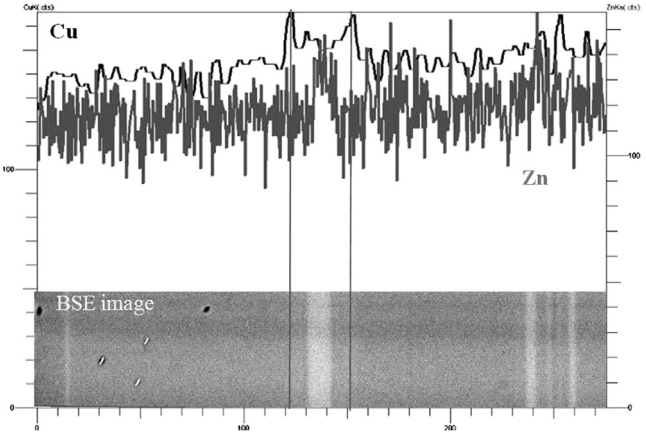

Fig. 8. Detail of Fig. 7 comparing X-ray line scans for Cu and Zn with BSE image. The position of the red striae in the glass is marked by the vertical lines lines.

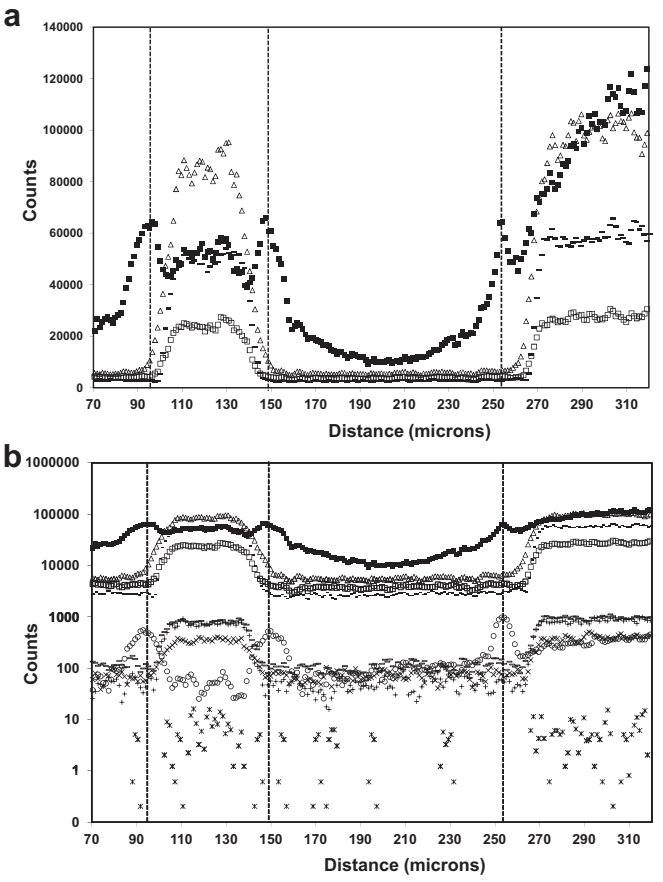

Fig. 9. a, b. LA-ICP-MS scan across the cross-section of red Type A shown in Fig. 6. a) linear scale showing detail of Cu, Zn, Sn, Pb. b) logarithmic scale comparing less abundant elements, note especially the coincidence of the behaviour of Ag with Cu. The approximate position of the red striae in the glass is marked by the vertical hatched lines.

the positions of the scans burned by the laser. Maxima in Cu concentration are observed in positions corresponding as far as can be discerned exactly to the red striae, and Ag mirrors this behaviour. Pb, Zn, Sn, As, In, Sb, and Au are higher in the Cu-rich glass but their behaviour with respect to the coloured zone differs from Cu and Ag. As in the X-ray linescan for Zn (Fig. 8), Pb, Zn, Sn, As, In and Sb are seen to fall sharply over a very short distance between the high-Cu and the low-Cu glass. Only Cu and Ag show secondary maxima in the area associated with the colour (Fig. 9a,b). Gold, which could be expected to behave similarly to Cu and Ag, is invariably present at sub-ppm levels, close to the detection limits, confirming that it does not play a significant role in the generation of the red colour.

High resolution SEM FEG observations of a number of *type A* reds show that copper in the vicinity of the striae is present as particles, some tens of nanometres in diameter (Fig. 10a, b, c). The nanoparticles are absent from the Cu-rich glass and occur only in the region of the Cu-poor glass adjacent to the Cu-rich glass.

As shown in Fig. 10a, the size of the nanoparticles is greatest in a thin region about 1 μm across. Depending on sample, it is located from a few μm up to perhaps a few tens of μm from the boundary between the two glasses; but always within the low-Cu glass. This zone of the coarsest nanoparticles corresponds to the layer of red colour seen in the optical microscope. Spacing of the nanoparticles in the coarse region is in the order of 500 nm (Fig. 10b). When the low-Cu layer was thin, the entire layer appears to have been accessible to copper which diffused from the high-Cu glass, so that

Table 3
Trace elements contents in ppm of red and white glasses in examples of Type A and Type B red glasses from York Minster.

	Glass layer	Cu	Zn	Pb	Sn	As	Ag	Sb	In	Au
Type A (York 11)	Colourless low-Cu[a]	826	460	129	103	4	0.5	1.2	0.7	–
	Colourless low-Cu[b]	1060	580	153	92	–	0.6	1	0.7	–
	Colourless high-Cu	15,200	3980	2320	1970	16	14	12.3	11	0.2
Type B (York 8)	Colourless low-Cu	434	309	44	2	–	0.4	0.4	0.5	0.004
	Red high-Cu	14,700	316	191	50	3	8	12	0.2	0.06

[a] Base glass.
[b] Low-Cu glass between high-Cu layers.

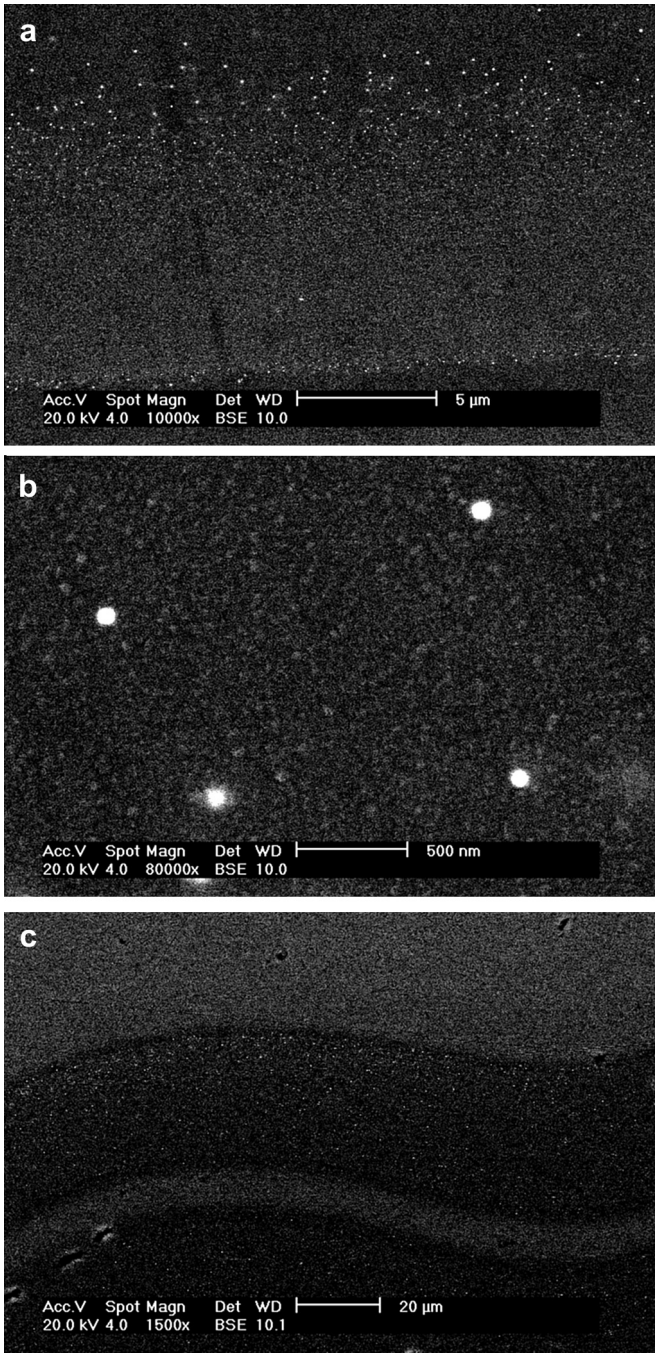

Fig. 10. a, b, c. BSE images of red type A (SEM FEG). (a) The dark grey area at the bottom of the image is high-Cu glass. Above this is the Cu-poor glass with a zone with precipitated nanoparticles, which become coarser away from the high-Cu glass. (b) detail of Cu nanoparticles. (c) sample from Canterbury showing undulating boundary.

Cu nanoparticles occur throughout the layer (Fig. 10c). However, red striae can be seen only within the narrow zone where the nanoparticles are sufficiently large.

The TEM imaging of a *type A* red from Burgos confirmed the SEM FEG findings and revealed more detailed characteristics of the Cu nanoparticles (Fig. 11). The particles are almost regularly spherical in shape. Their size increases progressively away from the high copper glass, in our example reaching about 35 µm. The area shown on Fig. 11 was divided into nine partially overlapping consecutive subareas (of about 12 × 9 µm). Fig. 12 depicts the area with the largest nanoparticles; only within the coarsest areas, could all nanoparticles be detected and measured, as the finest particles were not well resolved. Even allowing for an underestimation of the finest size fractions, the progressive increase in the number of particles in the finer areas, coupled with a reduction in spacing, is clear (Fig. 11). The smallest measurable particle was 1.5 nm, while the largest observed was 38 nm. The mean diameters for the consecutive areas increase from 5 to 28 nm. The EDS system attached to the TEM detected no copper in the glass between the coarsest particles.

An additional characteristic of some examples is the occurrence of florettes of a calcium phosphate phase in the nanoparticle-rich zone. The phase separation of calcium phosphate alongside

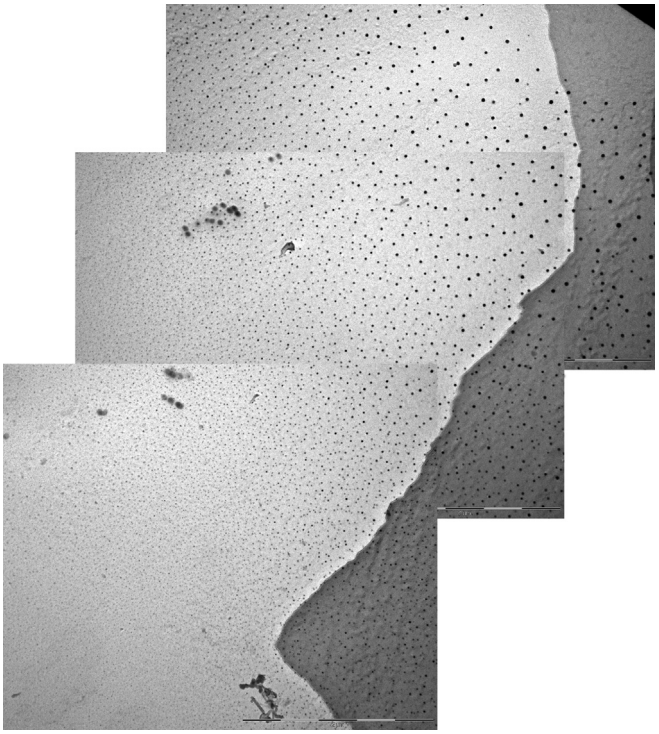

Fig. 11. Composite TEM image across a nanoparticle zone in red type A from Burgos, Spain, 13th century. Note the gradation in particle size from bottom left to top right.

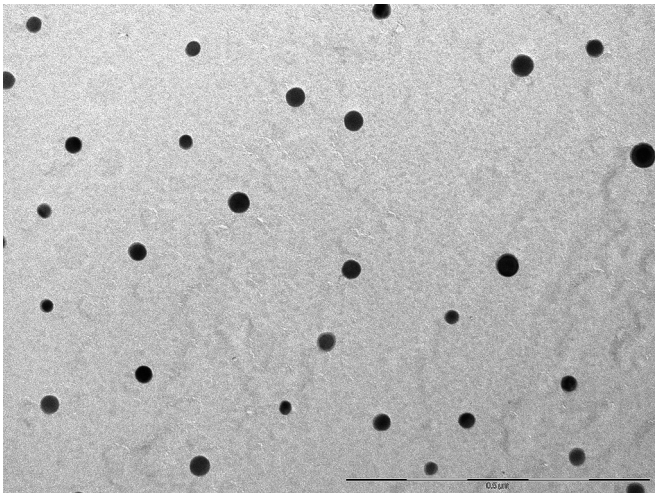

Fig. 12. Detail of largest copper nanoparticles in Fig. 11.

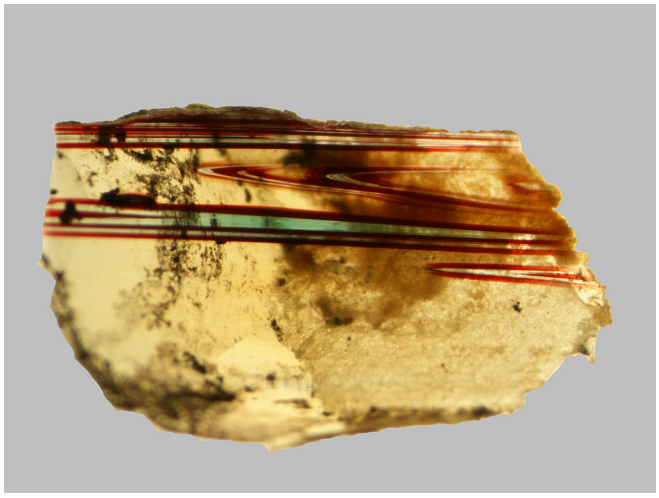

Fig. 13. A cross-section of red Type A with red striae folded and terminated unevenly. Bluish tint of some layers depicts the high-Cu glass; however this colour strongly dependant on observation angle. York Minster, New Clerestory, tracery, medallion panel (inv. no. C30 8T), probably 12th century. (For interpretation of the references to colour in this figure legend, the reader is referred to the web version of this article.)

metallic nanoparticles has also been observed in the glass of the Lycurgus Cup (Barber and Freestone, 1990).

Although the relation between structure, colour and composition is similar in all reds of *Type A* examined, there are some variations in the distribution of red striations. They may be densely packed and fill almost the entire cross-section of the glass sheet, may be more widely spaced and/or occupy only a limited portion of the cross-section of the sheet. Furthermore, striae are not invariably parallel or sub-parallel to the glass surfaces; they can also be folded and suddenly terminate (Fig. 13). The pattern of the red striae has a strong influence on the appearance of the glass to the viewer, so that folded striae seen in cross section can give rise to a 'wavy' pattern in the glass (Fig. 14). Most of the examples of such patterns, and all of those examined in detail here, are from the 12th century panels. These heterogeneities give a depth and texture to the reds which is a particularly appealing quality relative to later red glass.

To summarise, the foregoing observations indicate that:

(1) The *Type A* red glasses comprise alternate layers of a high-Cu and a low-Cu glass. These are not always parallel to the surface of the glass sheet.
(2) The red "stripes" in the glass are in fact very thin striations, only micrometres thick; previous reports of red layers of significant thickness are due to a failure to observe the glass parallel to the stripes, and the oblique view exaggerated their thickness.
(3) These striations form close to the boundary between the low-Cu and high-Cu glasses but within the low-Cu glass and do not correspond precisely to the boundary between them.
(4) The red striations appear as locally enhanced concentrations of copper. Microscopic observation confirms that the regions between the high-Cu glass and the red striae contain copper nanoparticles and these are coarsest where they correspond to the red colour.
(5) The high-Cu glass and the Cu-rich red zones in the low-Cu glass are likely to represent copper in two different oxidation states – in the high-Cu glass, the copper is dissolved and present as Cu^{+} and/or Cu^{2+} cations, while in the red zones in the low-Cu glass, the copper is present predominantly as metallic nanoparticles.
(6) While a range of metallurgically-related elements are associated with copper in the Cu-rich glasses, only silver shows similar maxima in concentration corresponding to the red striae.

3.2. Relation between structure, colour, and composition: Type B glass

Type B red glasses (Figs. 3 and 4) comprise a single red layer of finite thickness, on a colourless supporting sheet (2 layers – *Type B-2*), frequently protected by a covering layer (*coperta*) of white (3 layers – *Type B-3*). Colour is essentially homogeneous within the red layer and the striated appearance seen in *Type A* glasses is absent. The thicknesses of high-Cu red layers averages 104 μm in 35 samples of *B-2 type* (range 39–300 μm) and 114 μm in 51 samples of *B-3* glass (range 44–220 μm). The average thickness of the coperta layer on the *B-3* type is 127 μm. However the thickness varies greatly, ranging from 23 μm to 630 μm. This variation in thickness and the presence or absence of a covering layer may also reflect to some extent the degree of weathering and any cleaning of the glass surface that has been undertaken in the last century or so.

EDXA shows that the red layers are rich in copper relative to the accompanying colourless glasses. For 50 samples analysed by SEM-

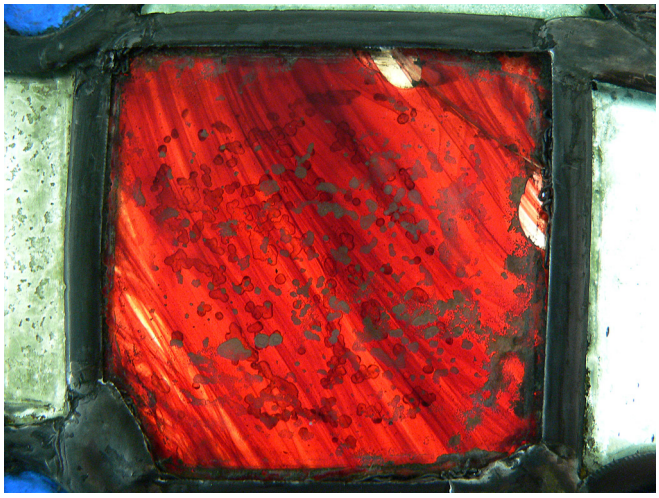

Fig. 14. In situ type A with 'wavy' pattern due to the uneven distribution of red striae. Canterbury cathedral, 12th century. (For interpretation of the references to colour in this figure legend, the reader is referred to the web version of this article.)

EDXA, CuO concentration in the high-Cu red layers varies between 0.8 and 2.4% with a mean of 1.6%. Average concentration of copper within the low-Cu layer was frequently below the detection limit of the EDXA system, but fourteen samples from York Minster (mainly 14th–15th century) and Fairford Church, Gloucestershire, UK (early 16th century) analysed by LA-ICPMS yielded a mean Cu content of 369 ppm (range 67 ppm–736 ppm).

Where the red is sandwiched between two colourless glass layers (*Type B-3*), these typically (but not invariably) have compositions identical within analytical error. Although Cu is sometimes found to be elevated in the outer layer, this appears to be due to the diffusion of Cu ions into the much thinner *coperta*.

The red and colourless layers typically differ significantly in a number of major and minor components, suggesting that the red glass is not simply the result of adding copper to the white, but that the base glasses (along with the *coperta* layers in *type B-3*) were made separately from the red. As a result of this, the high-Cu layer is typically readily distinguished in a back-scattered electron image. However, in a minority of examples the red glass appears to have been the result of adding copper to the white and apart from their contents of transition metals the red and white layers are identical (compositions of Type B supporting glasses and red layers are provided in Inline Supplementary Table 2).

Inline Supplementary Table S2 can be found online at http://dx.doi.org/10.1016/j.jas.2013.07.029.

The boundaries between the red and the white layers of *type B* glasses are sharply defined in back-scattered images. Line scans conducted on cross-sections demonstrate that the maxima observed on the copper diffusion profiles of *type A* glasses are not replicated in type B (Fig. 15). Cu, Pb, Sn, As, Ag, Sb, and Au decline gradually from red to colourless glasses. Typical concentrations of transition metal elements in both layers are shown in Table 3. Excluding copper, their total is extremely low in the low-Cu glass but is also not much higher in the high-Cu red glass.

High resolution SEM FEG of *Type B* glasses indicates that the nanoparticles are distributed only within and throughout the red layers, with sizes of a few tens of nm and spacing of from around a few tens to a few hundreds of nm (Fig. 16). In contrast to *Type A* glasses, they do not show any systematic variation in particle size with position in the red layer. Sparse crystals of calcium phosphate were sometimes observed on the boundary of the high-Cu and low-Cu glasses.

The TEM imaging (Fig. 17) of a red *Type B* from Holland (project sample no. 272) confirms the SEM FEG findings. For this sample, the average size of the nanoparticles within the high-Cu glass is

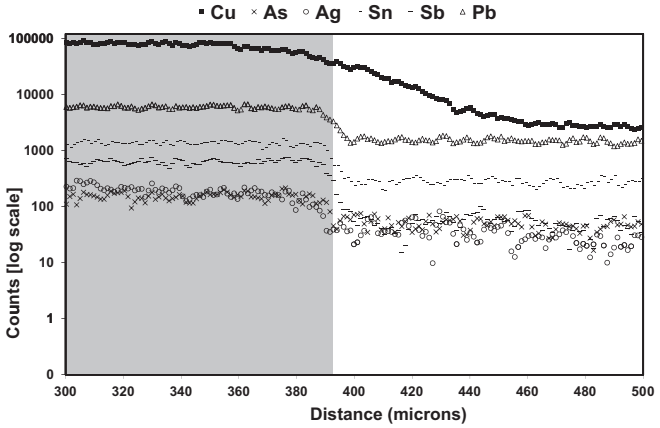

Fig. 15. LA-ICP-MS scan across cross-section of red type B. York Minster, Great East Window, panel 2b, sample R1. The occurrence of red colour is shaded.

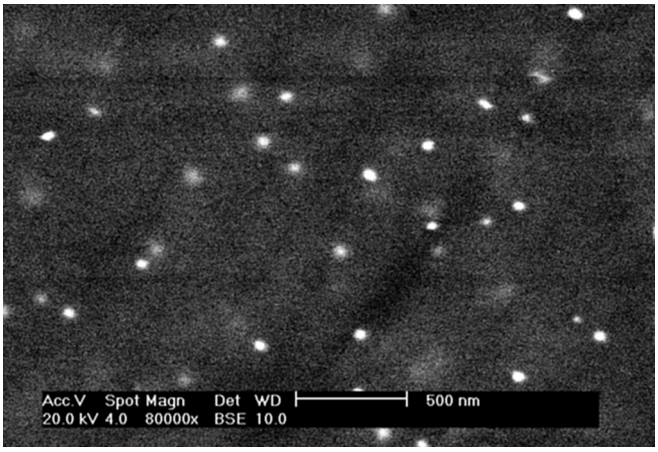

Fig. 16. Copper nanoparticles in type B high-Cu layer (BSE image, SEM FEG). Zuthpen, Holland.

22.4 nm ($s = 7.7$, min = 7.8, max = 37.4 nm, based on 90 measured particles). The TEM observation confirms their more-or-less random size distribution and that in a single glass, the average diameter is independent of the area examined. Ninety percent of the particles are between 10 and 35 nm. Only one nanoparticle was measured below 10 nm.

4. Discussion

4.1. Colour generation

We will consider first *Type B* glass, where microstructures and compositional variations are less complex. The nanoparticles responsible for the red colour have developed homogeneously within the Cu-rich glass layer and are not dependent upon inter-diffusion between the red and white glasses.

The size of the particles, at a few tens of nanometres, is broadly consistent with sizes for copper particles in glass stained with copper predicted by Mie's theory (Rawson, 1965; Bamford, 1977) and also with previous direct observation of copper nanoparticles in a sample of medieval red glass with Type B structure (Fredrickx, 2004; Fredrickx at al. 2005). They are slightly finer than the gold nanoparticles in the Lycurgus Cup, a rare example of Au-coloured Roman glass (Barber and Freestone, 1990) but are an order of

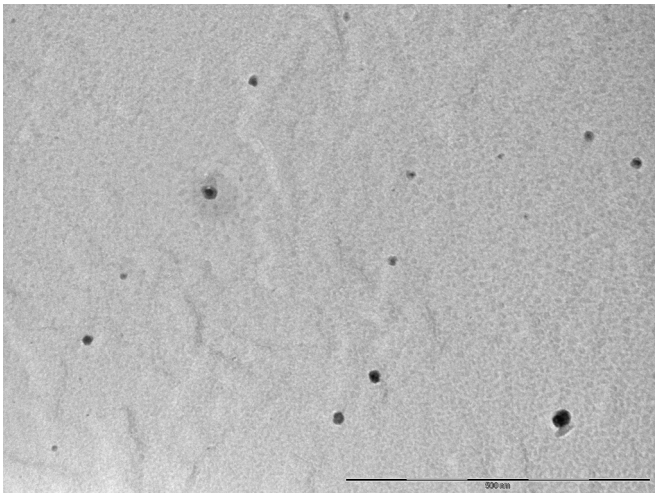

Fig. 17. TEM image of copper nanoparticles in glass type B from Zuthpen, Holland.

magnitude finer than the Cu-particles in the glazes of Chinese sacrificial red porcelain (Freestone and Barber, 1992) and opaque red Roman and Egyptian glasses (Brun et al., 1991; Barber et al., 2009) which approach micrometre-sized.

The Cu nanoparticles are likely to have developed by re-heating (heat-treating) the flashed glass after it was initially formed. The diffusion profiles observed across the boundaries between the red and white glasses are consistent with this interpretation, although they could also have developed at high temperatures when the white glass was coated with the red. In order for the copper to reduce to metal, there was a need for the Cu^{+} ions in the glass to gain an electron (Eq. (2)). In modern copper red glasses and glazes, the electron donor is typically a polyvalent cation such as Sn^{2+} (Ishida et al., 1987; Bring et al., 2007a,b):

$$2Cu^{+} + Sn^{2+} \rightarrow 2Cu^{0} + Sn^{4+} \quad (3)$$

However, tin and other polyvalent cations occur in very low concentrations in these medieval glasses. Therefore we must assume that the electron is donated by some other ion and ferrous iron appears to be the most likely candidate:

$$Fe^{2+} \rightarrow Fe^{3+} + e^{-} \quad (4)$$

Iron is naturally present in these glasses in concentrations of about 0.5%. The implication is that before the glasses were flashed, a substantial part of the iron and the copper were reduced to the Fe^{2+} and Cu^{+} states respectively. The attainment of this condition without an over-reduction of copper to metal is likely to have been challenging as the redox conditions of the ferrous–ferric oxide and copper–cupric oxide equilibria are close (Freestone, 1987).

The layered microstructures of *Type A* glasses are, as far as we are aware, unique and unrecorded in any other category of pre-modern glass. These characteristics resulted from the juxtaposition of two glasses, a low-copper and a high-copper glass, and the formation of Cu-nanoparticles in the low-copper glass as a result of diffusion from the adjacent high-copper material. Although low concentrations of a number of polyvalent ions, including Sn, Sb and As are present in the high copper glass, the compositional profiles indicate that they diffused more slowly into the low-Cu glass than copper. Moreover, their concentrations are very low and therefore they are unlikely to have had a significant role in the nucleation and growth of the metallic nanoparticles. The only available electron donor present in sufficiently high a concentration to allow the precipitation of the copper as metal appears again to have been ferrous iron (Equation (4)). Silver shows a similar compositional profile to copper and this is likely to reflect in part the monovalent states of both elements when dissolved in the glass, resulting in weaker bonds with the non-bridging oxygens of the silica network (O^{-}) than those of divalent elements such as zinc, so that they diffused more rapidly (Fig. 9a, b).

The absence of copper nanoparticles from the Cu-rich glass implies that here copper remained in its higher oxidation states, even when it was precipitating in the adjacent Cu-poor region. The essentially identical total iron contents of the high-Cu and low-Cu glasses imply that conversely the Cu-poor glass must have been reduced, with a significantly higher $Fe^{2+}/(Fe^{3+} + Fe^{2+})$ ratio, to cause the copper to precipitate. The sequence of events which resulted in the distribution of elements and nanoparticles seen in Figs. 8, 9 and 11 is illustrated schematically in Fig. 18 and was as follows:

1. An oxidised Cu-rich glass and a reduced Cu-poor glass were juxtaposed (in a manner discussed below).

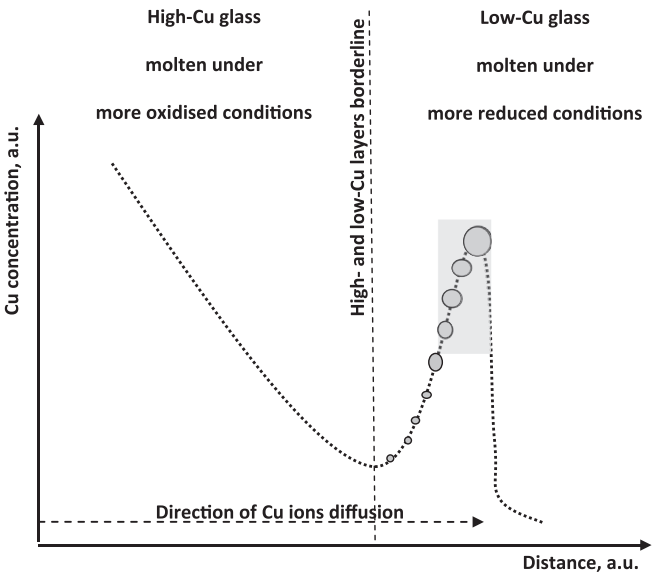

Fig. 18. Simplified scheme depicting the distribution, forms and concentration of copper across the red type A. Shading represents development of red colour.

2. The glasses were heat-treated allowing diffusion between them.
3. Cu^{+} and Ag^{+} ions, relatively loosely bound in the glass network due to their low field strengths, diffused relatively rapidly into the Cu-poor glass, while metallic elements of higher valency state diffused more slowly (Figs. 8 and 9). Note that because the major element compositions of the two glasses were essentially identical, no concentration gradient of standard glass-making components was observed.
4. As copper diffused into the reduced, low-Cu glass, it began to interact with the Fe^{2+} and reduced to Cu^{+} and/or Cu^{0}. At a distance of a few μm into the low-Cu glass, sufficient copper became reduced to allow the nucleation of metal particles. As heat-treatment continued, Ostwald ripening coupled with further diffusion of copper caused these particles to grow at the expense of finer particles, increasing the spacing between them and increasing their size so that they became large enough to cause a red colouration. This initial zone of nucleation and growth becomes the layer of coarse particles seen in the SEM and TEM (Figs. 10–12) and it corresponds to the maxima in the compositional profiles of Cu and Ag observed by EDXA and LA-ICPMS, as well as the line of intense colour seen in the light microscope (Figs. 2, 6, 8 and 9).
5. Nucleation and growth of nanoparticles occurred between the coarse layer and the Cu-rich glass, but because the reducing conditions were less strong (due to diffusion of oxidised copper) and the time for growth was shorter, these particles remained below the critical size needed to generate a ruby colour (Figs. 11 and 18).

Some observations of medieval cobalt blue glasses support the view that, under favourable conditions, nucleation of metallic copper can take place without the introduction of reducing agents in addition to the iron already present in the glass. Fig. 19 shows the cross-section of an example of such a cobalt blue glass with unintentionally developed red striations. Copper in medieval window glass is typically less than 200 ppm (unpublished work of the authors), but cobalt blue may contain up to 5000 ppm and, according to Weyl (1951) copper reds may develop in glasses with less than 2000 ppm Cu. In the example shown, the concentration of Cu

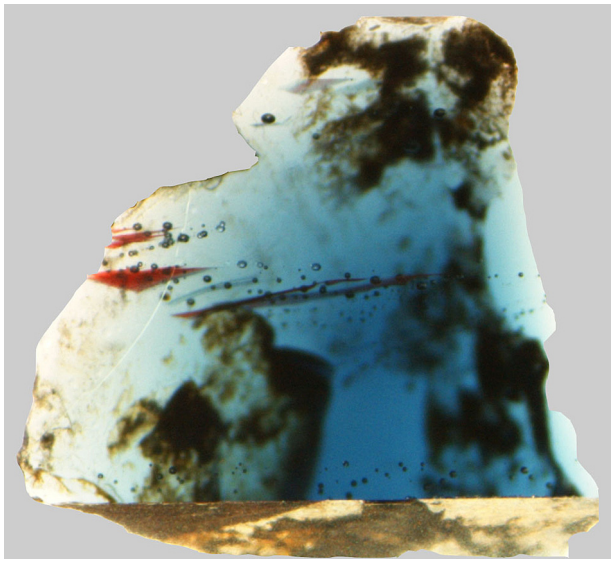

Fig. 19. Cobalt blue glass with localised development of red striae. Note associated bubbles. Great East Window, York Minster, panel 2h, sample B1. This HLLM type glass contains about 1060 ppm of Co and about 1740 ppm of Cu. (For interpretation of the references to colour in this figure legend, the reader is referred to the web version of this article.)

appears high enough to have resulted in precipitation of copper nanoparticles and the formation of red striations. There is a suggestion of a gradation in oxidation state from the strings of bubbles in the vicinity of the coloured regions. Unfortunately in this example the striae are embedded below the surface of the sample and are not easily accessible for detailed analysis.

4.2. Production technology

The morphology of *Type B* glass is very similar to that of modern flashed copper-red glass, where a thin layer of copper-bearing glass is achieved by dipping a gather of one colour into a pot of the other before blowing. Expansion of the glass into a cylinder by blowing caused thinning of the layers to the point where the red was translucent. Evidence that the red glass sheets under investigation were fabricated using the cylinder method is present on the (not grozed) edges of both Type A and Type B red glasses, which have rounded when the cylinder was heated and opened (Figs. 20 and 21).

In the typical medieval *Type B* red glasses, there are often significant compositional differences between the major element compositions of the red and white layers, implying the use of different batches of glass. Therefore it may be envisaged that the *Type B* glasses were often made using stock of two different batches: a white glass, and a red glass produced by oxidising and dissolving copper into a different batch of white glass. In the production of such a flashed red glass, a *coperta*, protecting the red glass from the air, is desirable to prevent reoxidation of the copper and loss of colour. To achieve such a protective covering layer of white, the gather was dipped into white glass a second time, after the red had been gathered, so that a sandwich was formed.

The copper in *Type B* glass was typically relatively pure, with only low levels of associated trace metals. It is likely that copper was added to the glass melt as oxide scale formed by heating copper sheet or filings. As noted above, the redox condition of the red glass had to be carefully manipulated so that it was favourable to the precipitation of copper nanoparticles on heat-treatment. Polyvalent ions such as tin and antimony are absent and there is

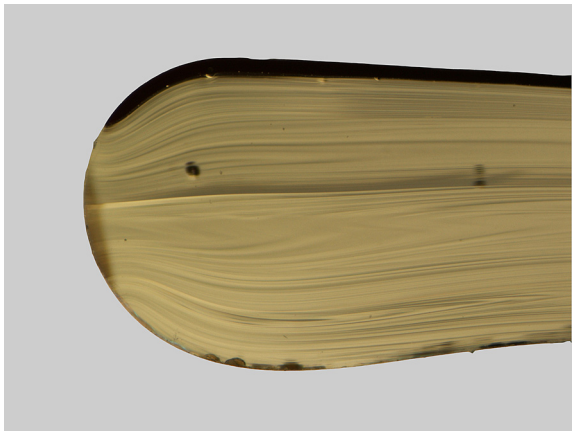

Fig. 20. Cross-section of an original, rounded (not grozed) edge (left hand side of photograph) of a red type B sheet from Zutphen (Dieserstraat), Netherlands. Certainly before 1572. Note pinched termination of red layer and evidence of distortion, consistent with the cutting of a cylinder and subsequent opening while hot, with rounding of edge. (For interpretation of the references to colour in this figure legend, the reader is referred to the web version of this article.)

no evidence for the addition of iron filings or iron scale to the red to act as a reductant. It is possible that the oxidation state of the melt was controlled by manipulation of the initial glass batch; the medieval treatise ascribed to Eraclius indicates that copper-red glass was made with "ashes not well baked" (Merrifield, 1849: 212–214), suggesting the presence of carbon to produce reducing conditions in the glass. Hawthorne and Smith (1963) point out that the sequence of colours reported by Theophilus to occur as medieval

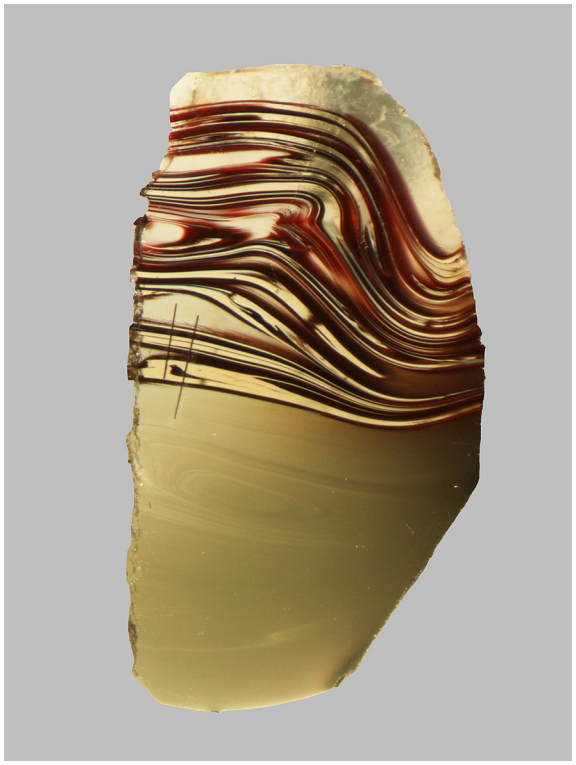

Fig. 21. Cross-section of an original, rounded (not grozed) edge (right hand side of image) of red type A from Chapter House (w1, window tracery), Canterbury cathedral, probably 14th century. Lines from laser scan may be observed centre left. (For interpretation of the references to colour in this figure legend, the reader is referred to the web version of this article.)

glass was melted are likely to have reflected the progressive oxidation of the glass in the kiln atmosphere. Selection of a glass which had been heated to an appropriate stage, or manipulation of the furnace atmosphere, were alternative approaches available to obtain an appropriately reduced glass.

Once the cylinder opened into a sheet it was transferred to an oven where it was heated until the copper struck and formed a red translucent layer. Fig. 22 presents a possible production sequence for reds of *Type B*, assuming a two-batch manufacturing process.

In *type A* glass, the copper appears to have been less pure than in *Type B*, perhaps reflecting the use of copper scale produced from recycled scrap rather than fresh copper stock. The concentrations of associated metals are high and suggest the use of scrap copper alloy as the copper source, corresponding – in the example given – to a quaternary Cu–Zn–Pb–Sn leaded gunmetal (Table 3). The base glasses for the white supporting layer, and the alternating high-Cu and low-Cu glasses were more often identical. Thus, in the production of a typical *Type A* red sheet, three pots of hot glass, usually derived from a single raw material and initially low in copper, appear to have been used. It seems likely that the initial batch was reduced in the first instance, perhaps through the use of "ashes not well baked" as prescribed by Eraclius (see above). If we assume that all three pots were held in covered pots or crucibles in a furnace at high temperature, then the first production step would have been to uncover Pot 3 and dissolve in the copper scale in by stirring and heating for a prolonged period in air, allowing it to oxidise and dissolve homogeneously. High-Cu glass from Pot 3 was then poured and stirred into Pot 2, containing the reduced low-Cu glass; this process was of short duration so that the two glasses were thoroughly interlayered but interdiffusion was minimised. A gather of white low-Cu glass from pot 1 was then dipped into the mixed glass in pot 2 and blown to produce a cylinder of low-copper white glass with a coating of mixed low- and high-copper glasses. The blowing process extended and thinned the layers in the mixed glass.

After opening the cylinder, the resultant sheet was placed in a kiln and heat-treated so that interdiffusion between the oxidised Cu-rich glass and the reduced low-Cu glass caused precipitation of copper nanoparticles in localised regions in the initial low-Cu glass and the development of thin striae of colour where the nanoparticles were largest. These layers were sufficiently spaced and thin that cumulatively they resulted in a translucent ruby effect. Key features of the chaîne opératoire for this glass are shown schematically in Fig. 23, assuming the use of a single initial glass batch. In principle, if the layers were sufficiently spaced, it would have been possible to produce a translucent red without a supporting white layer. However, we have not found a fully convincing example of such a structure. In our sample, in the majority of cases the sheet comprises a relatively thick supporting white layer, with a thinner overlying red.

Whereas in the *Type B* process, heat-treatment of the copper-bearing glass alone would have produced a dense or opaque red colour, it is noteworthy that none of the glasses used in the *Type A* process would have developed a red colour when cooled and heat-treated alone. The development of *Type A* red critically depended on the juxtaposition of an oxidised high-Cu glass, which is likely to have been pale blue or green when cool and a colourless reduced low-Cu glass. The knowledge needed to produce the red glass is likely to have been restricted to a relatively limited group of craftsmen, and the process of transformation of the two weakly coloured glasses into red must have appeared a marvel to the medieval artisans. The symbolic significance attached to the colour may have added to the impact of the transformation:- according to the future Pope Innocent III (1198–1216) red was the colour of blood, martyrdom and Christ's Passion.

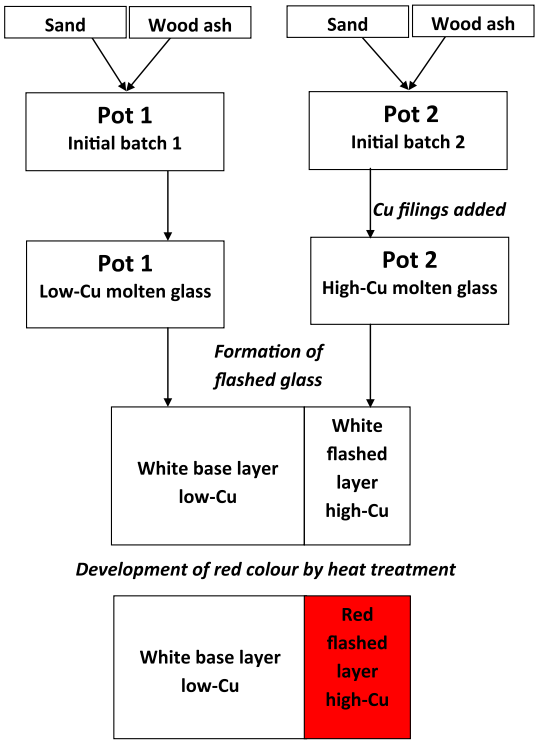

Fig. 22. Simplified scheme illustrating proposed manufacturing process of red Type B, assuming a two-batch manufacturing process. (For interpretation of the references to colour in this figure legend, the reader is referred to the web version of this article.)

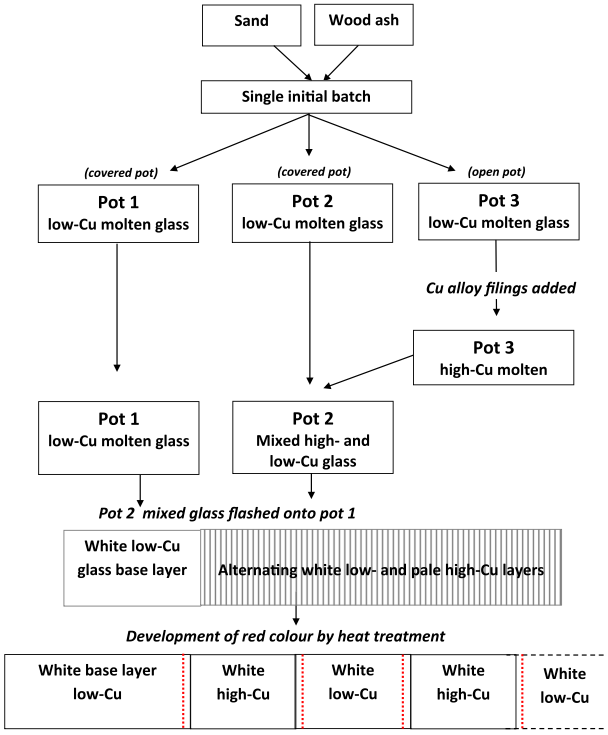

Fig. 23. Simplified scheme illustrating proposed manufacturing process of red Type A assuming a single-batch manufacturing process. (For interpretation of the references to colour in this figure legend, the reader is referred to the web version of this article.)

Multi-layered red glass of this type appears to have been otherwise unknown in the pre-industrial world and although the striated appearance was deliberately imitated by the American glass artist, Lawrence Saint in the 1930s and used by him in the Rose Window of Washington Cathedral (Saint, 1936, 1959), our ongoing investigations suggest that the technology differed in several respects. Japanese Satsuma glass of the 19th century also has red streaks but their compositional relationships are very different from those shown here (Nakai et al., 1999).

4.3. Chronology, innovation and change

The occurrence of the two glass types over time is summarised in Table 2 (for detailed information see Table 1). *Type A* appears to be restricted to the fourteenth century and earlier, while *Type B* occurs from at least the late fourteenth century. These findings are in line with the observations of Winston (1847) and Spitzer-Aronson (1974, 1975). However, it should be noted that we have examined in detail no red glasses pre-dating the fourteenth century from Germany, so cannot exclude the possibility that in fact the simple flashed *Type B* glasses were produced earlier in that region, rather than, or as well as, *Type A*. Indeed, K. H. Wedepohl (personal communication) informs us that he has not observed the *Type A* striated structure in any of his investigations of medieval glass from Germany, raising the possibility that this is a regional technological tradition, specific to southern and western Europe.

From the material we have examined in detail, largely from western Europe, we find a correspondence between *Types A* and *B* technology and the composition of the base glass, and this is largely a reflection of chronology. Fig. 5 shows that most *Type A* glasses are made using the earlier LLHM base type. A few *Type A* glasses group with the HLLM group in Fig. 5. However, these include: two samples from the Great West Window of Canterbury Cathedral, UK, which dates to 1396–1399, around the period of change between the two base glass types; a sample from Zutphen (Netherlands), which is of uncertain date ("probably fourteenth century") and finally a small group of twelfth century glasses from St Denis, France, but these also have the high potash contents (above 12%) which are characteristic of 12th–13th century reds and are therefore not typical HLLM glass. Moreover, a further characteristic of *Type A* reds is that all contain above 4.5% MgO; while all of *Type B* contain less than 5.5% MgO. Therefore the change from *Type A* to *Type B* red appears to have been more-or-less coincident with the change of base glass technology from LLHM to HLLM which occurred in the late 14th century.

One possible interpretation of the coincidence of the technological changes in base composition and red glass production technology is that there was an abrupt change in the source of supply of coloured glass and that HLLM glass and *Type B* technology were brought in together from an alternative workshop or production centre. A change of this type might have occurred due to social, economic or political upheavals, associated with major events such as the Black Death or the Hundred Years War. However, at around 1400, when base glass compositions changed, some *Type A* red was produced using the new HLLM glass, suggesting that the change from low lime to high lime glass preceded the change from *Type A* to *Type B* technology, if only by a relatively short period. In the absence of confirmatory data from a wider region, this conclusion must be tentative, but it appears that the change from *Type A* to *Type B* red glass technology may be dated to around 1400, following the change in base glass composition, and is not an apparent change due to a change in coloured glass supply. It seems that at this time, artisans who had been working to produce successful ruby red sheet glass in a centuries old tradition (*Type A* technology) made a deliberate choice to adopt a new approach.

Type B technology offers several advantages over *Type A*. In the first instance, workshop procedures required to produce *Type B* were less complex. Only two pots of hot glass, copper red and white, were required, as opposed to the three pots required for *Type A*. Furthermore, compositions indicate that *Type B* flashed and support layers were produced from different batches of glass, as opposed to the complex melting procedures involved in the production of *Type A*. Production of *Type A* also required the unpredictable mixing procedure of copper-bearing and copper-free glasses. This would have made *Type A* production difficult to control, as the thickness of the high- and low-Cu layers in the red glass depended upon a physical mixing process. The number of layers (hence red striae) varies significantly from sample to sample, and the intensity of the red colouration is likely to have varied within and between sheets.

On the other hand, *Type A* technology offered some advantages of its own. Firstly, the intercalation of red and colourless layers meant that the red colour was effectively protected from re-oxidation during manipulation of the hot glass by multiple *coperta* layers. Secondly, the colour-striking process is likely to have been less sensitive to variations in the oxidation state of the glasses. The nature of the diffusion-controlled colour formation process proposed is that provided the copper-poor glass was sufficiently reducing, copper would have precipitated at some point, and over- or under-reduction could have been compensated for by extending or reducing the duration of heat-treatment.

The relationship between total sheet thickness and the thickness of the white/colourless supporting layer is shown in Fig. 24. The immediate impression is the strong correlation between the total sheet thickness and the supporting glass for *Type B*. However, this is not surprising, as the red layers are very thin relative to the overall thickness of the sheets, so the two values plotted are almost identical for all *Type B* glasses. More significant is the distribution in the diagram of *Type A* glasses. It is observed that not only are the *Type A* red layers much thicker than *Type B*, but that their thickness varies markedly between samples, reflecting the problems with control that would have been encountered in their production.

The foregoing discussion suggests that there were technological advantages to the adoption of *Type B* red glass technology in terms of reduction in the complexity of production, i.e. time and labour input. Furthermore, the more predictable *Type B* process, once established, is likely to have required a lower level of tacit knowledge or skill, allowing easier transmission of the new technology between craftsmen, between workshops and between masters and apprentices.

Given the apparent advantages of *Type B*, it is perhaps surprising that *Type A* technology persisted for the preceding three centuries and that Type B was not developed sooner. This may be related to the arcane nature of *Type A* technology, involving the juxtaposition of oxidised and reduced glasses, neither of which would yield a red colour on its own; a high temperature partial mixing procedure of two essentially colourless glasses, where over-mixing would have resulted in no colour; followed by heat-treatment and striking of colour. The air of mystery surrounding the procedure, coupled with the marvellous transformation to red, must have reinforced the value of the resulting ruby glass, which was intended for use in a sacred context and, as noted above, had a powerful symbolic significance. Any advantage in production efficiency may well have been outweighed by the potential loss of such intangible benefits. Furthermore, as observed by Saint (1936, 1959), the multi-layered character of *Type A* glass, where the reds have a depth and texture not produced by the simple flashed layer of *Type B*, is much more pleasing to the modern eye. Whether this particular aesthetic also appealed to the medieval mind is unclear, however.

Whatever the reason for the persistence of *Type A* technology, the relatively abrupt change to *Type B* appears to have closely

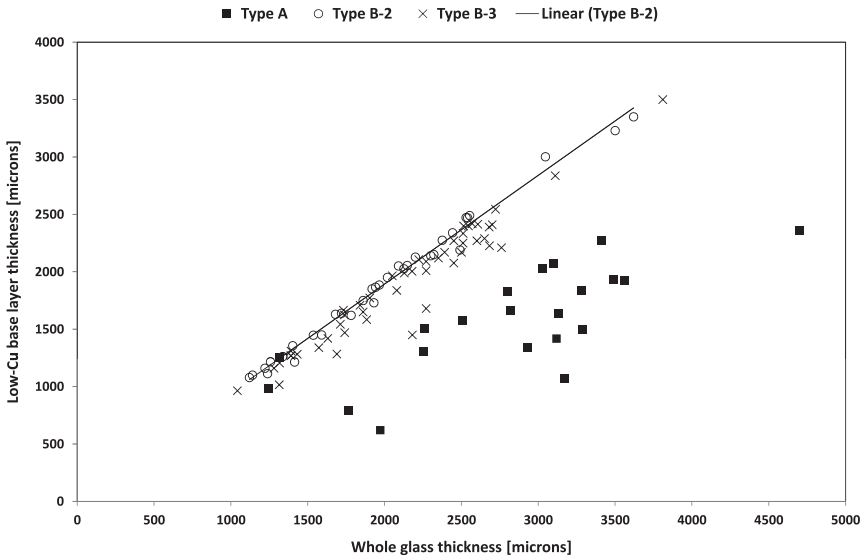

Fig. 24. Relation between thickness of the low-Cu base white glass and the whole glass sheet thickness for the red glass types ($n = 102$ – includes only the samples where the thickness could be measured).

followed on from the change in base glass compositions from low- to high-lime. Basic principles suggest that this would have involved changes in glass melting and working properties; lower glass viscosities, for example, might have favoured the production of Type B reds. Furthermore, these changes imply modifications in other workshop practices such as furnace design and operation. The change from *Type A* to *Type B* red glass production technology therefore occurred at a time of experimentation and other changes in the production of coloured window glass are likely to have led to a more receptive and open approach to the way colours were made. If we assume, following Eraclius (Merrifield, 1849: 212) that ashes used in glassmaking were a mixture those derived from both fern and wood (cf. Tennent et al., 1984; Smedley et al., 2003), then the increasing lime content and reduction in potash would reflect a lower content of fern ash, which was relatively uneconomical to harvest on a large scale (Jackson and Smedley, 2006). Coupled with the reduction in copper contents of the *Type B* glasses and the reduced labour input needed to produce them, the overall trend may seen to be one of increased control over product and reduction in cost. Therefore we may see the displacement of *Type A* by *Type B* glass as part of a move to more productive working practices in glass technology and away from technological preferences centred on tradition, belief and mystery, which were rooted in the medieval view of the world.

The development of *Type A* technology appears to have derived from the glassmaking practices of late antiquity and the early medieval period. Particularly from the eighth century CE, the re-use of old Roman coloured glass, procured in the form of opaque mosaic tesserae, appears to have been widespread. This continued through into the production of enamels and window glass in the twelfth century, as explained by Theophilus (Hawthorne and Smith, 1963) and illustrated by the investigation of a wide range of artefacts (e.g. Biron et al., 1996; Biron and Beauchoux, 2003; Freestone, 1992, 1993; Wolf et al., 2005). While the production of translucent cobalt-blue or copper-green glass would have been easily attained by mixing Roman opaque glass with soda- or potash-based colourless glass and dispersing the colourant ions, the production of translucent copper-red glass was not possible in this way, due to the oxidation and dissolution of the copper particles. Hence, earlier attempts to produce red glass vessels and sheets which transmit some light appear to involve incomplete mixing of opaque red and colourless glass to give streaks of opaque red in a translucent green or colourless glass matrix (e.g. Baumgartner and Krueger, 1988; Evison, 2000). This practice of partially mixing glasses is likely to have led to the discovery of *Type A* technology. However, the generation of *Type A* red may have originated in the mixing of a pre-existing oxidised copper blue or green glass with a colourless glass rather than the re-use of an opaque red. The mixing of a Roman copper blue (as opposed to a cobalt blue) with a medieval potash glass, which was reduced to the use of incompletely ashed wood (see above), could have resulted in a *Type A* red. Mixing of soda-rich Roman glass with medieval potash glass should therefore be sought in the reds of the earliest stained glass windows.

5. Conclusions

Medieval red window glass is invariably coloured by copper nanoparticles and there is no evidence for a role of gold in the colouration. The red sheets fall into two types: a simple flashed layer of red glass on a white (colourless) base, typically covered with a thin white *coperta* layer (*Type B*), and a multilayered variety (*Type A*) which was used only in windows pre-dating about 1400 AD.

Many earlier studies of medieval red window glass appear to have assumed that the earlier multi-layered *Type A* glasses represent alternate layers of red and white glass (Alonso et al., 2009; Farges et al., 2006; Ortega-Feiu et al., 2011). Careful microscopic observations have shown that this is not the case, and that the red colouration is concentrated in thin streaks or striae just a few micrometres thick. The glasses are compositionally layered, but the striae do not conform to the boundaries between the layers. Instead they formed due to diffusion of copper across the layer boundaries from an oxidised copper-bearing glass into a reduced copper-free glass. Copper nanoparticles nucleated at a critical intersection of compositional and oxidation gradients along the diffusion profile. The layered glasses are not formed by folding, as has been suggested (Farges et al., 2006), but by a process of partially mixing, gathering and blowing into a cylinder. The latter process stretched the relatively thick layers in the gather into thin alternating laminae in the glass sheet.

As far as we are aware, the technology we have inferred for *Type A* glass was unknown from the early fifteenth century until the

twentieth century and perhaps until the present day. This study represents the rediscovery of this medieval technique by archaeometric analysis. Thanks to modern methods of microscopy and analysis we have been able to discern the significance of features which was not possible in the earlier studies of Spitzer-Aronson.

The technology, involving the juxtaposition of a colourless and a pale blue or green glass to produce a red colour must have made a great impression on the medieval observer and could have been understood at only the most empirical level. The complex and arcane procedures involved are likely to have ensured that red glass production was confined to a small number of glass glassmakers working in a closed tradition. It is likely to have ensured that the production of red glass was the monopoly of a restricted number of workshops.

The production model outlined here will be amenable to testing by the use of X-ray absorption spectrometry to measure the relative oxidation states of the glass layers. These measurements are already under way. Furthermore, it is necessary to expand the coverage of our survey to include 12th–14th century glasses from churches in modern Germany and Austria. This will determine the relationship between *Type A* and *Type B* technologies more clearly and allow us to understand the origins of the two approaches. If it is demonstrated, as we suspect, that Type A glass is not found in Germany, the structure of red glass will offer a straightforward approach to determine whether glass has originated in German or French glass houses. We also plan to investigate the twentieth century reproductions of medieval red glass by Laurence Saint, as his windows and his notebooks suggest that he came closer than any other to replicating the medieval approach.

This new understanding of medieval red glass has implications for work in a number of areas, including the investigation of chronology and the glass trade. An understanding of the compositions of the surface layers of red glass will also help to explain its corrosion and differences in deterioration between red glasses of the thirteenth and fourteenth centuries. It will also allow improved replication and restoration of medieval windows by allowing the production of more authentic materials showing similar light transmission behaviour. Finally, this study provides a link between the glass colouring practices of the later first millennium and the high medieval period, and a pathway for the development of stained glass window technology.

Acknowledgements

This work was funded by a Leverhulme Trust Project grant to I C Freestone and T Ayers. The experimental measurements were carried out while Kunicki-Goldfinger and Freestone were members of the School of History and Archaeology, Cardiff University and we thank Phil Parkes for his help in maintaining the SEM. An anonymous referee made helpful comments and suggestions on the manuscript. We thank Professor K.H. Wedepohl for many helpful discussions on the chemistry of medieval glass. We are grateful to the following colleagues and institutions for access to glass in their care: The Dean and Chapter of York Minster; Mr Nick Teed and the York Glaziers Trust; Ms Sherrie Eatman from the Victoria and Albert Museum; Mr Keith Barley of Barley Studio, York; Drs David Saunders and Catherine Higgitt of the Department of Conservation and Science of the British Museum; Ms Léonie Seliger, Canterbury Cathedral Studios; Ms Ulrike Brinkmann, Cologne Cathedral, Germany; Oidtman Conservation Studio, Linnich, Germany; Mr Mike Stansbie, Coventry Cathedral, UK; Ms Abigail Hykin and Dr Richard Newman of the Museum of Fine Arts, Boston, USA; Mr Roen van Gulik from the Archeologische Wergroep Beverwijk-Heemskerk, Holland; Mr Michel Groothedde and Ms Dineke van Krimpen, Collection of Gemeente Zutphen, Holland; Mr Michael Hulst from Gemeente Amsterdam, Holland; Ms Elżbieta Gajewska-Prorok of the National Museum in Wrocław, Poland; Ms Agnieszka Gola and Dr Jerzy Ilkosz, The Director of the Museum of Architecture in Wrocław, Poland; Mr Sławomir Oleszczuk, Wroclaw, Poland; Mr Fernando Cortes Pizano, Alicante, Spain and Dr Francisco Capel del Aguila, Instituto de Cerámica y Vidrio, Consejo Superior de Investigaciones Cientificas, Spain.

References

Alonso, M.P., Capel, F., Valle Fuentes, F.J., De Pablos, A., Ortega, I., Gómez, B., Respaldiza, M.A., 2009. Caracterización de un vidrio rojo medieval procedente de las vidrieras del Monasterio de las Huelgas de Burgos. Boletin de la Sociedad Española de Cerámica y Vidrio 48, 179–186.

Bamford, C.R., 1977. Colour Generation and Control in Glass. Elsevier, Amsterdam.

Barber, D.J., Freestone, I.C., 1990. An investigation of the origin of the colour of the Lycurgus Cup by analytical transmission electron microscopy. Archaeometry 32, 33–45.

Barber, D.J., Freestone, I.C., Moulding, K.M., 2009. Ancient copper red glasses: investigation and analysis by microbeam techniques. In: Shortland, Andrew J., Freestone, Ian C., Rehren, Thilo (Eds.), From Mine to Microscope. Advances in the Study of Ancient Technology. Oxbow, Oxford, pp. 115–127.

Baumgartner, E., Krueger, I., 1988. Phoenix aus Sand und Asche. Glas des Mittelalters. Munich.

Biron, I., Beauchoux, S., 2003. Ion beam analysis of Mosan enamels. Measurement Science and Technology 14, 1564.

Biron, I., Dandridge, P., Wypyski, M., 1996. Techniques and materials in Limoges enamels. In: Boehm, B.D., Taburet-Delahaye, E. (Eds.), Enamels of Limoges 1100–1350. Metropolitan Museum of Art, New York, pp. 48–62.

Brill, R.H., 1999. Chemical Analyses of Ancient Glass. Corning Museum of Glass, Corning, N.Y.

Brill, R.H., Cahill, N.D., 1988. A red opaque glass from Sardis and some thoughts on red opaques in general. Journal of Glass Studies 30, 16–27.

Bring, T., Jonson, B., Kloo, L., Rosdahl, J., Wallenberg, R., 2007a. Colour development in copper ruby alkali silicate glasses. Part 1. The impact of tin (II) oxide, time and temperature. Glass Technology: European Journal of Glass Science and Technology, Part B 48, 101–108.

Bring, T., Jonson, B., Kloo, L., Rosdahl, J., 2007b. Colour development in copper ruby alkali silicate glasses. Part 2. The effect of tin (II) oxide and antimony (III) oxide. Glass Technology: European Journal of Glass Science and Technology, Part B 48, 142–148.

Brun, N., Mazerolles, L., Pernot, M., 1991. Microstructure of opaque red glass containing copper. Journal of Materials Science Letters 10, 1418–1420.

Chopinet, M.-A., 2004. Evolution des alcalins dans les mélanges vitrifiables depuis le 18e siècle. Verres 9, 38–45.

Clow, A., Clow, N.L., 1952. The Chemical Revolution. A Contribution to Social Technology. The Batchworth Press, London.

Colomban, Ph., Tournié, A., Riccardi, P., 2009. Raman spectroscopy of copper nanoparticle-containing glass matrices: ancient red stained-glass windows. Journal of Raman Spectroscopy 40, 1949–1955.

Cramp, 2001. Window glass from the British Isles, 7th–10th century. In: Dell'Acqua, F., Silva, R. (Eds.), Il Colore Nel Medioevo – La Vetrata in Occidente dal IV al'XI Secolo. Lucca, pp. 67–85.

Dell'Acqua, F., Silva, R., 2001. Il Colore Nel Medioevo – La Vetrata in Occidente dal IV al'XI Secolo. Corpus Vitrearum Medii Aevi Italia, Lucca.

Evison, V.I., 2000. Glass vessels in England AD 400–1100. In: Price, J. (Ed.), Glass in Britain and Ireland AD 350–1100, London, British Museum: Occasional Paper 127, pp. 47–104.

Farges, F., Etcheverry, M.-P., Scheidegger, A., Grolimund, D., 2006. Speciation and weathering of copper in "copper red ruby" medieval flashed glasses from the Tours cathedral (XIII century). Applied Geochemistry 21, 1715–1731.

Fredrickx, P., 2004. Transmission Electron Microscopy for Archaeo-Materials Research: Nanoparticles in Glazes and Red/Yellow Glass and Inorganic Pigments in Painted Context (PhD Thesis). Universiteit Antwerpen, Faculteit Wetenschappen, department Fysica, Antwerp.

Fredrickx, P., De Vis, K., Wouters, H., Hélary, D., Schryvers, D., 2005. Nanoparticles in glass and glazes. In: Art'05 – 8th International Conference on 'Non Destructive Investigations and Microanalysis for the Diagnostics and Conservation of the Cultural and Environmental Heritage', Lecce (Italy), May 15th–19th 2005, p. 14. CD-ROM, Paper No. B-016.

Freestone, I.C., 1987. Composition and microstructure of early opaque red glass. In: Bimson, M., Freestone, I.C. (Eds.), Early Vitreous Materials, London: British Museum Occasional Paper 56, pp. 173–191.

Freestone, I.C., 1992. Theophilus and the composition of medieval glass. In: Vandiver, P.B., Druzik, J.R., Wheeler, G.S., Freestone, I.C. (Eds.), Materials Issues in Art and Archaeology III, Pittsburgh: Materials Research Society Symposium Proceedings, vol. 267, pp. 739–746.

Freestone, I.C., 1993. Compositions and origins of glasses from Romanesque champleve enamels. In: Stratford, N. (Ed.), Catalogue of Medieval Enamels in the British Museum. Volume II Northern Romanesque Enamel. British Museum Press, London, pp. 37–45.

Freestone, I., Barber, D., 1992. The development of the colour of sacrificial red glaze with special reference to a Qing Dynasty Saucer Dish. In: Scott, R.E. (Ed.), Chinese Copper Red Wares. Percival David Foundation of Chinese Art, London, pp. 53–62.

Freestone, I.C., Stapleton, C.P., Rigby, V., 2003. The production of red glass and enamel in the Later Iron Age, Roman and Byzantine periods. In: Entwistle, C. (Ed.), Through a Glass Brightly – Studies in Byzantine and Medieval Art and Archaeology Presented to David Buckton. Oxbow, pp. 142–154.

Freestone, I., Kunicki-Goldfinger, J., Gilderdale-Scott, H., Ayers, T., 2010. Multidisciplinary investigation of the windows of John Thornton, focusing on the Great East Window of York Minster. In: Shepard, Mary B., Pilosi, Lisa, Strobl, Sebastian (Eds.), The Art of Collaboration: Stained-Glass Conservation in the Twenty-first Century. Harvey Miller, Turnhout, pp. 151–158.

Gao, S., Liu, X., Yuan, H., Harttendorf, B., Gunther, D., Chen, L., Hu, S., 2002. Determination of forty two major and trace elements in USGS and NIST SRM glasses by laser ablation-inductively coupled plasma-mass spectrometry. Geostandards Newsletter 26, 181–196.

Goll, J., 2001. Frühmittelalterliche Fenster Gläser aus Müstair und Sion. In: Dell'Acqua, F., Silva, R. (Eds.), Il Colore Nel Medioevo – La Vetrata in Occidente dal IV al'XI Secolo, pp. 87–98. Lucca.

Hawthorne, J., Smith, C.S., 1963. Theophilus on Divers Arts. University of Chicago Press.

Ishida, S., Takeuchi, N., Hayashi, M., Wakamatsu, M., 1987. Role of Sn^{4+} in development of red colour during reheating of copper glass. Journal of Non-Crystalline Solids 95 & 96, 793–800.

Jackson, C.M., Smedley, J., 2006. Medieval and post-medieval glass technology: bracken as a sustainable resource in medieval glassmaking. Glass Technology: European Journal of Glass Science and Technology Part A 47 (2), 39–47.

Knowles, J.A., 1927. The history of copper ruby glass. Transactions of the Newcomen Society for the Study of the History of Engineering and Technology 6, 66–74.

Merrifield, M.P., 1849. Medieval and Renaissance Treatises on the Arts of Painting. John Murray, London. Dover Replica Edition 1967.

Nakai, I., Ch., Numako, Hosono, H., Yamasaki, K., 1999. Origin of the red color of satsuma copper-ruby glass as determined by EXAFS and optical absorption spectroscopy. Journal of the American Ceramic Society 82, 689–695.

Newton, R.G., 1977. Simulated medieval glasses. Corpus Vitrearum Newsletter 25, 3–5. Available at: http://www.corpusvitrearum.org/.

Ortega-Feliu, I., Gómez-Tubío, B., Respaldiza, M.A., Capel, F., 2011. Red layered medieval stained glass window characterization by means of micro-PIXE technique. Nuclear Instruments and Methods in Physics Research B 269, 2378–2382.

Rawson, H., 1965. The calculation of transmission curves of glass stained by copper and silver compounds. Physics and Chemistry of Glasses 6, 81–84.

Roe, M., Plant, S., Henderson, J., Andreescu-Treadgold, Brown, P.D., 2006. Characterisation of archaeological glass mosaics by electron microscopy and X-ray microanalysis. Journal of Physics: Conference Series 26, 351–354.

Saint, L., 1936. Is stained glass a lost art? Bulletin American Ceramic Society 15, 375–382.

Saint, L., 1959. The romance of stained glass. Huntingdon, Pa.: privately mimeographed. Reproduced as 'Excerpts from the Romance of Stained Glass by Lawrence Saint'. Journal of the British Society of Master Glass-Painters 16 (1976–1977), 11–30.

Smedley, J.W., Jackson, C.M., Welch, C., 2003. Unravelling Glass Compositions: detecting the Use of Specific Glassmaking Raw Materials at Little Birches, Staffordshire. Annales du 15e Congrès de l'Association Internationale pour l'Histoire du Verre, pp. 203–207.

Spitzer-Aronson, M., 1974. La distribution du cuivre dans les verres rouges des vitraux médiévaux. Comptes Rendus – Académie des Sciences, Paris 278 (17 juin 1974), 1437–1440 série C.

Spitzer-Aronson, M., 1975. Étude de vitraux rouges médiévaux à l'aide de microscope optique, microscope à balayage avec image par électrons rétrodiffusés et microsonde électrique à rayons X. Verres et Réfractaires 29, 145–153.

Spitzer-Aronson, M., 1976. Contribution à la connaissance des vitraux du Moyen Age. Insuffisance de la diffusion pour expliquer la non-concordance stricte entre la presence de cuivre et la couleur à l'intérieur des verres des vitraux rouges. Verres et Réfractaires 30, 56–61.

Spitzer-Aronson, M., 1977. Vers une meilleure connaissance d'un métier d'art médiéval. Étiude de plusieurs procédés modernes pour reproduire des verres rouges feuilletés des vitraux du Moyen Age. Verres et Réfractaires 31, 25–31.

Spitzer-Aronson, M., 1978a. Physique et recherche fondamentale au service de l'histoire des vitraux médiévaux. Annales du 7e Congés de l'Association Internationale pour l'Histoire du Verre, Berlin-Leipzig 15–21 Août 1977, Edition du Secretariat General a Liege, pp. 309–320.

Spitzer-Aronson, M., 1978b. Nouvelles méthodes non destructives destinées à la recherche fondamentale sur les vitraux médiévaux. Silicates Industriels 10, 213–218.

Spitzer-Aronson, M., 1979. Précision sur les techniques médiévales des vitraux par des recherches en physique. Verres et Réfractaires 33, 26–34.

Spitzer-Aronson, M., 1980. A new method for the study of flat glasses microstructure implications of trace elements variation on the structure of glasses. Journal of Non-Crystalline Solids 42, 601–606.

Spitzer-Aronson, M., 1989. Analytical and historical research on medieval multilayered copper-red glass. In: Maniatis, Y. (Ed.), Archaeometry. Proceedings of the 25th International Symposium. Elsevier, pp. 671–676.

Tennent, N.H., McKenna, P., Lo, K.K.N., McLean, G., Ottaway, J.M., 1984. Major, minor and trace element analysis of medieval stained glass by flame atomic absorption spectrometry. In: Lambert, J.B. (Ed.), Archaeological Chemistry III. American Chemical Society, Washington D.C, pp. 133–150.

Verità, M., Santopadre, P., 2010. Analysis of gold-coloured ruby glass in Roman church mosaics of the fourth to 12th centuries. Journal of Glass Studies 52, 11–24.

Vicenzi, E.P., Eggins, S., Logan, A., Wysoczanski, R., 2002. Microbeam characterization of corning archaeological reference standards: new additions to the Smithsonian Microbeam Standard Collection. Journal of Research of the National Institute of Standards and Technology 107, 719–727.

Wedepohl, K.H., 2003. Glas in Antike und Mittelalter. Geschichte eines Werkstoffs. E. Schweizerbart'sche Verlagsbuchhandlung, Stuttgart (Nägele u. Obermiller).

Wedepohl, K.H., 2010. The manufacture of medieval glass. Glassmaking in Europe between A.D. 500 and 1500. In: Whitehouse, D. (Ed.), Medieval Glass for Popes, Princes, and Peasants. The Corning Museum of Glass, Corning, New York, pp. 63–69.

Weyl, W.A., 1951. Coloured Glasses. Society of Glass Technology, Sheffield, U.K.

Whitehouse, D., 2001. Window glass between the first and the eighth centuries. In: Dell'Acqua, F., Silva, R. (Eds.), Il Colore Nel Medioevo – La Vetrata in Occidente dal IV al'XI Secolo, pp. 31–43. Lucca.

Winston, C., 1847. An Inquiry into the Difference of Style Observable in Ancient Glass Paintings. John Henry Parker, Oxford.

Wolf, S., Kessler, C.M., Stern, W.B., Gerber, Y., 2005. The composition and manufacture of early medieval coloured window glass from Sion (Valais, Switzerland)—a Roman glass-making tradition or innovative craftsmanship? Archaeometry 47, 361–380.